Discrete Modeling of Deformation of Glassy Amorphous Polymers

A Thesis Submitted in Partial Fulfillment of the Requirements for the Degree of

Master of Technology

by

Manish Mukherjee

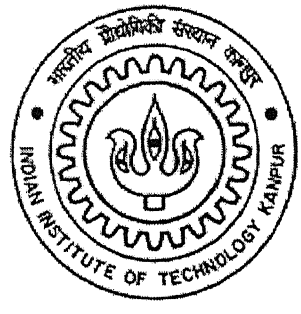

to the

DEPARTMENT OF MECHANICAL ENGINEERING
INDIAN INSTITUTE OF TECHNOLOGY KANPUR
INDIA

August, 2004

CERTIFICATE

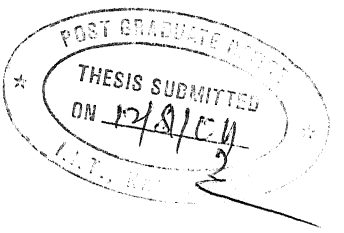

This is to certify that the work under the thesis titled **Discrete Modeling of Deformation of Glassy Amorphous Polymer** by **Manish Mukherjee (Roll No. Y210519)** has been carried out under my supervision and this work has not been submitted elsewhere for a degree.

August, 2004

Dr. Sumit Basu
Department of Mechanical Engineering,
Indian Institute of Technology
Kanpur.

Dedicated to

My Beloved Parents

Acknowledgement

I would like to take this opportunity to express my deep sense of gratitude to my thesis supervisor Dr. Sumit Basu, for his invaluable guidance and relentless encouragement. It would have never been possible for me to take this thesis work to completion without his support and encouragement. His systematic approach to all matters has been a significant influence on my way of working. I am certainly fortunate to get a chance to work under him. I am thankful especially for his constant support and guidance on personal level.

The fantastic atmosphere and cooperation extended by my labmates, Yogesh, Dhiraj, and Rabindra helped to make this thesis work a unforgettable experience.

I would like to thank all my friends for all the cherishable moments, support and help they extended to me during my stay at IIT Kanpur. The life here would not have been so memorable without my great friends, particularly Yogesh, Arvind, Vikram, Shrikant and Nilesh. Special thanks must be given to Yogesh Kanaujia for his help and support during my stay at IIT campus.

I would like to thank my parents for taking me to this stage of life; it was their blessings and sacrifices which always gave me encouragement to face all challenges and made my path easier.

And above all, I thank the Almighty for enabling me to achieve higher goals.

Manish Mukherjee

Abstract

In this work we perform discrete modeling and analysis of the deformation of glassy amorphous polymer. Amorphous polymers consist of long molecular chains that are randomly oriented. Modeling of these chains is done by using a coarse grained self avoiding random walk (SAW) model. A chain generated by SAW can not cross itself but two chains can pass through a common position in space called the entanglement point. This simulates the effect of entanglements on the deformation. Care is taken to avoid a particular chain from overlapping another chain. Chains are obtained in a regular grid of dimensions obtained from specifications of the polymer under study.

The final polymer model is like a nonlinear truss and the analysis of this structure takes account of material and geometric non-linearities. The constitutive response of the members of the truss is like rubber elasticity obeying Langevin statistics. Total Lagrangian formulation is applied to the model which uses the Second Piola-Kirchoff stress and the Green Lagrange strain tensor.

Finite element analysis of the truss structure is done to obtain stress-strain curves.

This model is capable of providing quantitative information on

(1) stress-strain behavior, molecular extension ,chain fracture and slippage

(2) importance of the molecular weight and its distribution

(3) effects of testing variable, such as temperature and strain rate.

Contents

CHAPTER 1: INTRODUCTION

Now a days polymers are widely used in various fields, such as structures, composites etc. The most important aspect of polymer material is the diversity of accessible molecular composition, as well as a choice of monomers. Establishing a good connection between molecular composition and material properties is a difficult task due to complex structural and dynamic features observed in these materials. Our work will be based on predicting a model and simulating it to get the properties of polymer under study. In particular it is concentrated to get stress-strain curve to predict the mechanical properties of amorphous polymers.

Polymers consist of large molecules i.e. macromolecules. A monomer is the repeating unit of which a polymer is made of, for e.g. propylene is the monomer which polymerizes to give polypropylene. Polymer crystals show direction-dependent (anisotropic) properties. For e.g. Young's modulus of polyethylene in chain direction at room temperature is 100 times of the Young's modulus in transverse direction, this difference in modulus is due to the presence of two types of bond present in the crystal: 1) strong and stiff bond along chain axis and 2) weak and soft secondary bond acting in the transverse direction. However these weak (Van der Waals) bonds are also present with strong bonds along chain axes.

When a polymer is cooled down from molten state it either crystallizes or cools down to its glassy amorphous state as shown in Figure 1. The temperature at which the slope in volume-temperature graphs changes is referred as glass transition temperature, T_g. Basically the chains in amorphous polymers are randomly oriented and that of crystalline polymers are oriented in a regular fashion. In our work we had used the kinetic model developed by Termonia and Smith. [1,2] for tensile deformation of amorphous polymers. This model is based on Eyring Activation rate theory [3] and classical theory of rubber elasticity [4].

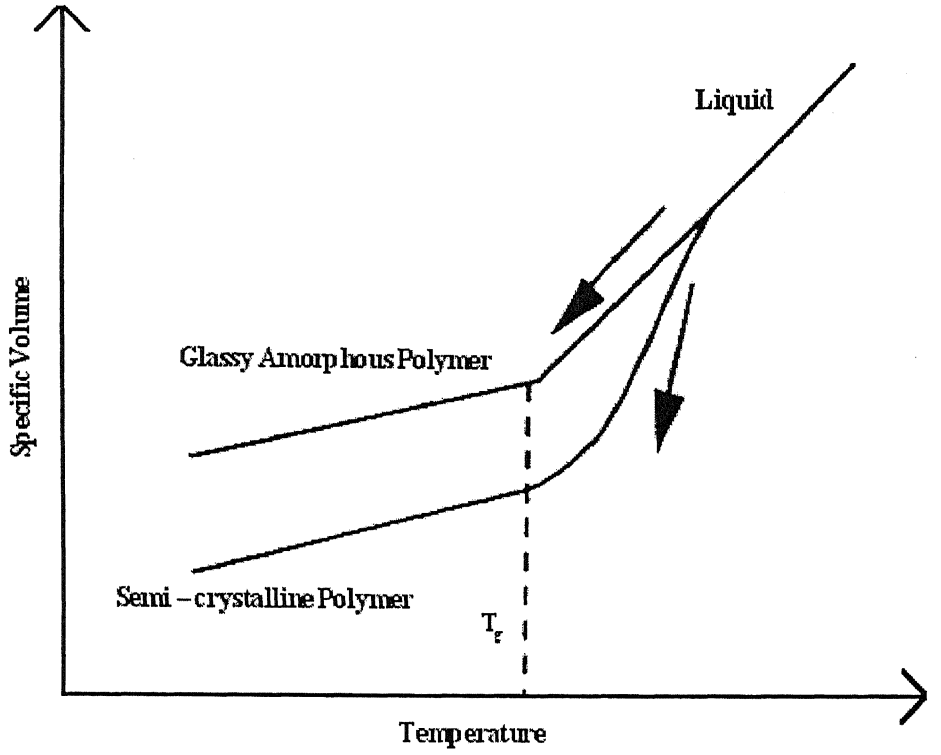

Figure 1 Cooling of molten polymer

1.1 Comparison with other models:

The macroscopic or bulk models take into account the overall stress-strain behavior of a polymer and not local stress-strain variation which occurs at microscopic or atomistic levels. On the other hand atomistic models consider individual atoms and bonds explicitly which makes the study of large system almost impossible. The model which we are using considers the local extension ratios and stresses of chain strands by applying the concepts of rubber elasticity theory to each individual rubbery chain strands and linear elasticity theory to weak Van der Waals bonds. The chain segment between two entanglement points contain hundreds of atoms in rubbery phase, therefore the model is neither macro nor atomistic but is mesoscopic. This model a) includes the most relevant details in simulations of mechanical properties of polymer and b) keeps the computer time and memory requirements within acceptable limits.

The model is capable of giving information on

1) Stress-Strain behavior based on molecular extension, chain fracture and slippage.
2) Effect of testing variables, such as temperature and strain rate.

3) Importance of molecular weight and its distribution.

1.2 Literature Survey:

Our model is based on the work done by Termonia and Smith [1]. Many models have been developed to describe phenomenon like brittle fracture, yielding, strain hardening etc [4]. This model is based on Eyring activation rate theory [3] which takes into account weak attractive forces between chains and also chain slippage through entanglements. According to our model the weak Van der Waals bonds break according to the kinetic theory of fracture [5]. The stresses in the strands are obtained using the classical theory of rubber elasticity [4]. The simulation of Van der Waals bond breaking is performed with the help of Monte Carlo lottery procedure developed by Termonia [1].

The theory of Rubber Elasticity was developed by Meyer, Von Susich and Valko [4] and Karrer [4]. Karrer developed the concept of Brownian motion at various portion of long chain molecule structure. Meyer, Von Susich and Valko considered the relation between elasticity and the ability of chain to take up an irregular or statistically determined form by virtue of the interchange of energy between its constitutive elements and surrounding atom. This is fundamental concept of now theory of rubber elasticity.

Busse [6] considered the general condition necessary for rubber like elasticity and gave the concept that rubber like elasticity is associated with micro-Brownian motion of individual element of long chain molecules. Later on this concept helped to develop the concept of Van der Waals bonds in polymer structure.

When the kinetic theory of elasticity was first proposed Meyer and Ferri [4] realized the importance of variation of elastic tension with temperature i.e. deformation is entropy driven. In the absence of external forces the chain molecules will adopt configurations corresponding to a state of maximum entropy (contracted configuration of chain). When forces are applied the chains will tend to extend in the direction of the force, so reducing the entropy and produce a state of strain. Our model is based on random walk, and the solution to random walk (chain) problem was first given by Kuhn [7] and by Guth and

Mark [8]. The problem consists of essentially in evaluating the relative number of configuration of the chain, for given values of x, y and z or getting the information on the probability of a chain having a particular end-to-end length.

Statistical theory of a polymer network is first proposed by Kuhn [7] who showed that the elastic modulus could be directly related to the number of molecules per unit volume of material. Later on Wall [4], James and Guth [13], James [10], Treloar [11] made their contribution to statistical theory of rubber elasticity which was based on Gaussian statistics. Later on non-Gaussian Statistical network theory was developed which takes into account the finite extensibility of the chain and hence of the network. Kuhn and Grun [12] gave the idea of statistical treatment of random chain by non-Gaussian statistical network theory. They used the inverse Langevin function to get an expression for probability of a chain having a particular end-to-end distance. James and Guth [13] used the inverse Langevin distribution function to give expression for the force per unit area.

1.3 Overview of the Work:

Present work is an attempt at predicting the mechanical behavior of glassy amorphous polymers from a mesoscopic perspective. Modeling of amorphous polymer chains is done by using a coarse grained self avoiding random walk (SAW) model. The final polymer model is like a nonlinear truss and the analysis of this structure takes account of material and geometric non-linearities. Total Lagrangian formulation of truss is done based on the Second Piola-Kirchoff stress and the Green Lagrange strain tensor. The polymer model is assumed to behave according to the laws of rubber elasticity. Finally strain energy-strain and stress-strain curves were obtained for the polymer model.

CHAPTER 2: RUBBER ELASTICITY

2.1 Introduction:

In this work we intend to build a lattice based, mesoscopic model of deformation. This model will be based on the statistical theory of rubber elasticity. Analogy will be drawn between the affine deformation of networks of rubber macromolecules and plastic deformation of amorphous polymers. This analogy is motivated by the work of Arruda and Boyce [14] and Wu and Van der Giessen [15] on constitutive models of glassy polymers.

2.2 Statistical properties of long chain molecules:

The Theory of Rubber Elasticity on the basis of structural and thermodynamic concepts is developed in two stages:

1) Development of mathematical expressions for probability and entropy as function of end to end distance.
2) Treating network of such long chain molecules by statistical methods.

Ensemble of random chains can only be described by means of a spatial distribution function. A random chain is shown in Figure 1.

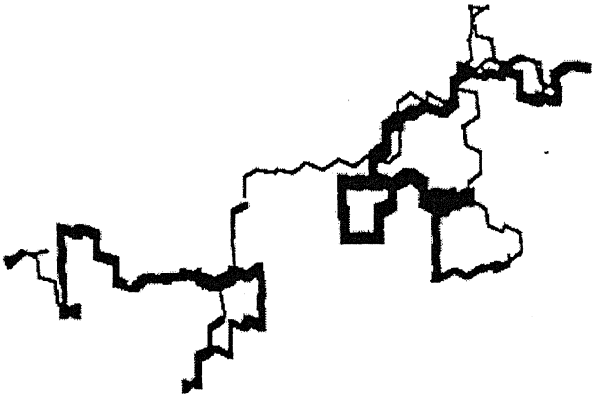

Figure 2 Random chain

The end-to-end distance(r) and the radius of gyration(s) are two different measures of random chain. The former is the distance between the chain ends and the latter is the root mean square distance of the collection of atoms from there common center of gravity. The following relation holds good between r and s.

$$< s^2 >=< r^2 > / 6 \qquad (1)$$

2.3 End-to-end distance of a macromolecular chain:

Average end-to-end distances of long macromolecular chains can be calculated using various levels of approximations. A polymer molecule in a 'theta' solvent (solvent that does not cause the coil to either expand or shrink) follows the equation:

$$< r^2 >_0 = Cnl^2 \qquad (2)$$

Where the subscript '0' signifies the theta condition, n is the number of chain links in a particular chain and l is the length of each link and < > signifies average over the value. The constant C depends on the nature of the polymer. This formula considers only the short range interactions. If the long range interaction are considered then,

$$< r^2 >= \alpha^2 < r^2 >_0 , \qquad (3)$$

where α is the expansion factor and is affected by temperature and type of solvent.

2.4 Models for calculation of average end-to-end distances:

Some models for calculation of end-to-end distance of molecular chain are as follows

1) Freely jointed chain:

For a freely jointed chain with main chain bonds (segments) each bond having length l, it can be shown that,

$$< r^2 >= nl^2 . \qquad (4)$$

In this approximation it is assumed that the orientation of the individual segments is totally uncorrelated. See Figure 2.

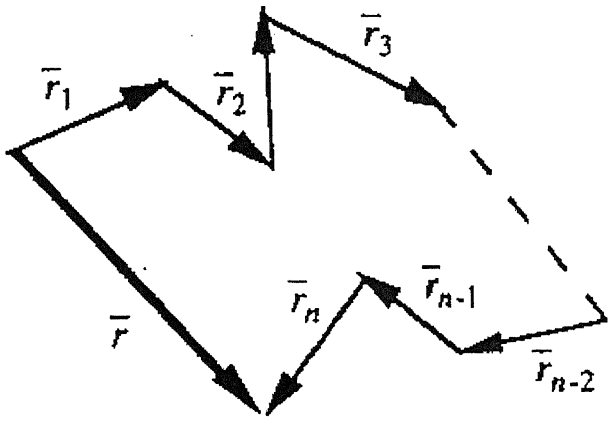

Figure 3 Freely jointed chain

2) Freely rotating chain:

A freely rotating chain model assumes that the bond angle θ is a constant. No particular chain conformation is preferred and the average projection of bond i+1 along a direction perpendicular to bond i is zero. Taking $\theta \approx 110^{o}$ this assumption yields,

$$< r^2 > \approx 2nl^2 . \qquad (5)$$

It is assumed that each C-C bond permits of free rotation, so that, for example, the bond C_2C_3 may be considered to rotate about C_1C_2 as axis, while C_3C_4 rotate about C_2C_3 as axis, and so on.

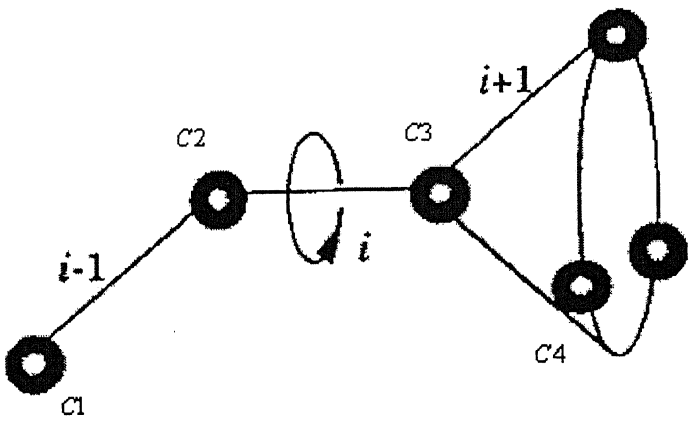

Figure 4 Freely rotating chain

3) Hindered rotation chains:

Above models neglect any hindrances to rotation. They assume that all positions of rotating bond are equally possible, it doesn't respond to conditions in actual molecular chain where attractive and repulsive forces between atoms of neighboring chains makes certain positions of rotation more probable. These effects are conveniently described in terms of difference in potential energy between different positions.

For example ethane ($CH_3 - CH_3$), where hydrogen atoms repel each other causing energy maxima in eclipsed position and minima in staggered position. For this model

$$< r^2 >= nl^2[\frac{1+\cos(\pi-\theta)}{1-\cos(\pi-\theta)}][\frac{1+<\cos\phi>}{1-<\cos\phi>}]. \qquad (6)$$

For freely rotating chain model, $<\cos\phi>= 0$. For higher alkanes the quantity $<\cos\phi>$ can be obtained from consideration of the existence of trans and gauche states. $<\cos\phi>$ is function of potential energy and temperature , as temperature increases potential becomes less effective and RMS length tends to approach that of unrestricted rotation.

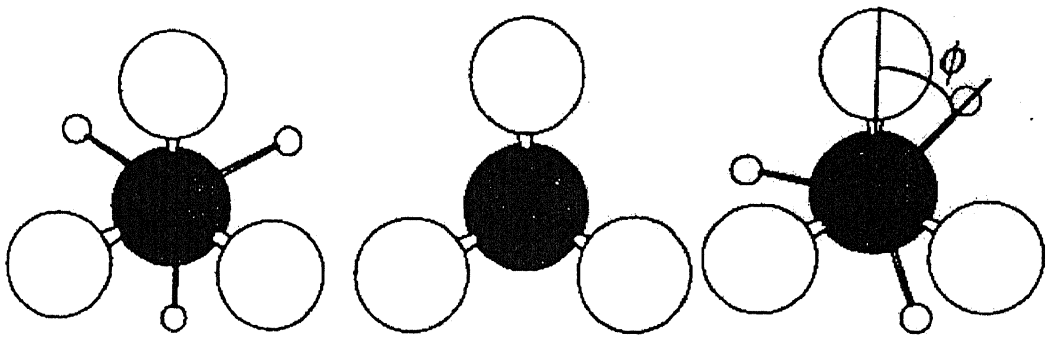

Staggered position (most stable) | Eclipsed position (least stable) | Intermediate position, definition of torsion angle(ϕ)

Figure 4 Rotational isomers of ethane from a view along the C-C bond: carbon-shaded; hydrogen-white

4) Concept of an equivalent chain:

The constant C in equation (2) arises from short range interactions. We can actually assume an equivalent chain comprising of N' hypothetical segments each of length l', so that the equivalent chain behaves like a freely –jointed chain with

$$< r^2 >= N'l'^2 \tag{7}$$

$$\text{and} < r_{max} >= N'l' . \tag{8}$$

Thus for real polymer with $r_{max} = 0.83Nl$ and $< r^2 >_0 = 6.7Nl^2$, with $N/N' \approx 10$, this means that each segment of the equivalent chain consists of 10 real bonds. In other words, the actual chain orientation becomes uncorrelated after every 10 bonds.

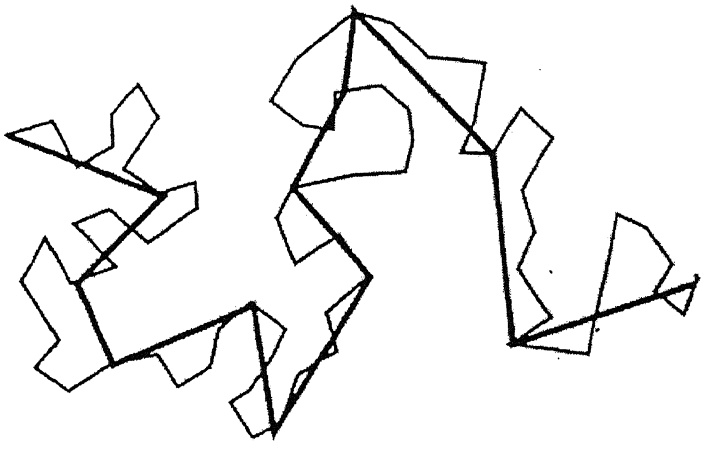

Figure 5 Equivalent chain

2.5 Distribution of end-to-end vectors:

The distribution of end-to-end vectors for Gaussian chains follows the distribution function:

$$P(x,y,z)dxdydz = \left(\frac{3\pi}{2\pi < r^2 >_0}\right)^{3/2} \exp\left[-\frac{3(x^2+y^2+z^2)}{2 < r^2 >_0}\right] dxdydz \tag{9}$$

Where $< r^2 >_0$ is the average end-to-end distance of the chain. The above formula gives the probability of finding the chain, whose origin is at (0, 0, 0) at the point (x, y, z). This formula is strictly true for any chain that can be represented as a hypothetical equivalent chain with n freely jointed chain, each having length (l) as explained above.

2.6 Rubber Elastic State:

2.6.1 Introduction:

Unlike in metals elasticity exhibited by rubbers is entropy-driven. This is demonstrated by the thermo-elastic effects: a) stretched rubber subjected to uniaxial load contracts reversibly on heating; and b) rubber gives out heat reversibly when stretched. This confirms the fact that entropy of rubber decreases on stretching. This behavior is different from energy driven or energy elasticity of metals, ceramics.

2.6.2 Thermodynamic consideration:

To illustrate the contrast between energy and entropy elasticity thermodynamic relations are set for stretching of a sample uniaxialy. According to the first law of thermodynamics the energy change, dE, for a body subjected to a transfer of heat, dQ, and change in volume, dV, under pressure P and uniaxial deformation is given by

$$dE = dQ - PdV + fdL, \tag{10}$$

where f is the retractive force and dl is the change in length, l, of the sample. For the reversible case TdS = dQ, and so

$$dE = TdS - PdV + fdL. \tag{11}$$

We define Gibbs free energy (G) as:

$$G = H - TS, \tag{12}$$

Where the enthalpy H is given by,

$$H = E + PV. \tag{13}$$

Hence

$$dG = dE + PdV + VdP - TdS - SdT. \tag{14}$$

From (10) and (13)

$$dG = fdL + VdP - SdT. \tag{15}$$

Thus we have

$$\left(\frac{\partial G}{\partial L}\right)_{p,T} = f \text{ and} \tag{16a}$$

$$\left(\frac{\partial G}{\partial T}\right)_{L,p} = -S . \tag{16b}$$

Since the order of differentiation is unimportant:

$$\left(\frac{\partial}{\partial T}\left(\frac{\partial G}{\partial L}\right)_{p,T}\right)_{p,L} = \left(\frac{\partial}{\partial L}\left(\frac{\partial G}{\partial T}\right)_{L,p}\right)_{p,T}, \tag{17}$$

implying

$$\left(\frac{\partial f}{\partial T}\right)_{L,p} = -\left(\frac{\partial S}{\partial L}\right)_{p,T} . \tag{18}$$

Partial derivative of G with respect to L at constant P and constant T is given by:

$$\left(\frac{\partial G}{\partial L}\right)_{p,T} = \left(\frac{\partial H}{\partial L}\right)_{p,T} - T\left(\frac{\partial S}{\partial L}\right)_{p,T} . \tag{19}$$

Combining equations (18) and (19) gives:

$$f = \left(\frac{\partial H}{\partial L}\right)_{p,T} + \left(\frac{\partial f}{\partial T}\right)_{p,L}, \tag{20}$$

The first term in rhs of the above equation can be written as

$$\left(\frac{\partial H}{\partial L}\right)_{p,T} = \left(\frac{\partial E}{\partial L}\right)_{p,T} + \left(\frac{\partial V}{\partial L}\right)_{p,T} . \tag{21}$$

Now assuming that volume is constant during deformation i.e.

$\left(\frac{\partial V}{\partial L}\right)_{p,T} \approx 0$, we have

$$\left(\frac{\partial H}{\partial L}\right)_{p,T} = \left(\frac{\partial E}{\partial L}\right)_{p,T} . \tag{22}$$

And so we have equation for force as

$$f = \left(\frac{\partial E}{\partial L}\right)_{p,T} + T\left(\frac{\partial f}{\partial T}\right)_{p,L} . \tag{23}$$

The first term in the equation (23) is associated with change in internal energy accompanying deformation at constant pressure while the second term accounts for the change in entropy by deformation as:

$$\left(\frac{\partial f}{\partial T}\right)_{p,L} = -\left(\frac{\partial S}{\partial L}\right)_{p,T} \tag{24}$$

from (18).

So equation (23) shows that the total force has an energetic and an entropic term. The entropic part, in case of polymers arises from the changes in chain orientations accompanying deformation.

2.6.3 The Statistical Mechanical Theory of Rubber Elasticity:

To develop the concept of Statistical Mechanical Theory of Rubber Elasticity we have to go through the concept of affine and phantom models. In affine deformation model the junction points are assumed to have fixed positions defined by deformation ratio, while the chains between junction points are free to take any possible conformation. The junction points of phantom network are allowed to fluctuate about their mean position and the chains between these junction points can take great many possible conformations. Statistical Mechanical theory starts from affine network model which obeys following assumptions;

1) The chain segments between crosslinks are represented by Gaussian statistics of phantom chains.
2) The entropy of the network is the sum of the entropies of the individual chains which are N in number per unit volume.
3) The deformations on the molecular level are the same as that on a macroscopic level, i.e., deformation is affine.
4) The unstressed network is isotropic.
5) The volume remains constant during deformation.

The distribution of end-to-end vectors is as follows from (9)

$$P(x,y,z)dxdydz = \left(\frac{3\pi}{2\pi < r^2 >_0}\right)^{3/2} \exp\left[-\frac{3(x^2+y^2+z^2)}{2 < r^2 >_0}\right] dxdydz .$$

Entropy is given by the equation

$$S = k \ln P , \tag{25}$$

and so

$$S = k\left\{\frac{3}{2}\ln\left(\frac{3\pi}{2\pi < r^2 >_0}\right) - \frac{3(x^2+y^2+z^2)}{2 < r^2 >_0}\right\}.$$

Therefore

$$S = C - k\frac{3r^2}{2 < r^2 >_0}, \tag{26}$$

where C is a constant; k is the Boltzmann's constant.

An unstressed chain is represented by end-to-end vector starting at the origin and having position vector $\bar{r}_0 = (x_0, y_0, z_0)$ and end-to-end vector $\bar{r} = (x, y, z)$ corresponds for position vector of stressed state and is related to $\bar{r}_0$ through $(\lambda_1, \lambda_2, \lambda_3)$ by relations:

$$x = \lambda_1 x_0 \quad y = \lambda_2 y_0 \quad z = \lambda_3 z_0$$

The change in entropy of the chain due to this stretch is given by

$$\Delta S_N = \sum_1^n \Delta S = -3k\left(\frac{\left(\lambda_1^2 - 1\right)x_0^2 + \left(\lambda_2^2 - 1\right)y_0^2 + \left(\lambda_3^2 - 1\right)z_0^2}{2 < r^2 >_0}\right). \tag{27}$$

Here the change in entropy for the network is the sum of the contributions of all the chain segments of the network.

It is assumed that original system is isotropic i.e.

$$\begin{aligned}
&\sum_1^N x_0^2 = \sum_1^N y_0^2 = \sum_1^N z_0^2 \\
&\sum_1^N x_0^2 + \sum_1^N y_0^2 + \sum_1^N z_0^2 = \sum_1^N r_0^2 \\
&\sum_1^N x_0^2 = \sum_1^N y_0^2 = \sum_1^N z_0^2 = \frac{1}{3}\sum_1^N r_0^2 = \frac{N < r^2 >_0}{3}
\end{aligned} \tag{28}$$

where N is the number of Gaussian chain segments in the system. From equation (27) and (28) we have entropy change for network as:

$$\Delta S_N = -\frac{1}{2}kT(\lambda_1^2 + \lambda_2^2 + \lambda_3^2 - 3).$$

Consequently the change in internal energy is given by

$$\Delta G = -T\Delta S_N = -\frac{1}{2}NkT(\lambda_1^2 + \lambda_2^2 + \lambda_3^2 - 3).$$

Assuming volume to be constant during deformation we get:

$$\lambda_1\lambda_2\lambda_3 = 1. \tag{29}$$

For uniaxial stress deformation with

$\lambda_1 = \lambda$, we have from (29)

$$\lambda_2 = \lambda_3 = \frac{1}{\sqrt{\lambda}}, \text{ where } \lambda = \frac{L}{L_0}.$$

Here L is the current length in x_1 direction in which the original length was L_0.

Using equation (16a) we get

$$f = \left(\frac{\partial G}{\partial L}\right)_{T,V} = \frac{\partial G}{\partial \lambda}\frac{\partial \lambda}{\partial L} \qquad \text{implying}$$

$$f = \frac{NkT}{L_0}\left(\lambda - \frac{1}{\lambda^2}\right). \tag{30}$$

Cauchy stress is obtained using $A = A_0 / \lambda$ (A is the area of cross section of specimen):

$$\sigma = \frac{\lambda f}{A_0} = nRT\left(\lambda^2 - \frac{1}{\lambda}\right), \tag{31}$$

where n is the number of moles of Gaussian chain segment and V_0 is the volume of specimen. Also n/ V_0 can be expressed as:

$$\frac{n}{V_0} = \frac{nM_c}{V_0}\frac{1}{M_c} = \frac{\rho}{M_c},$$

where M_c is the molecular weight of each Gaussian segment. Hence

$$\sigma = \frac{\rho RT}{M_c}\left(\lambda^2 - \frac{1}{\lambda}\right). \tag{32}$$

The rubber modulus $C_R = \frac{\rho RT}{M_c}$ is linearly dependent on temperature and inversely proportional to.

2.6.4 Drawbacks of classical statistical theory and implementation of non-Gaussian statistical theory:

Gaussian statistics is good approximation only if end-to-end distance is considerably smaller than chain length (*Nl*). Non-Gaussian statistical treatment takes into account the finite extensibility of the chain, and thus leads to a more realistic form of distribution function which is valid over the whole range of r values up to the fully extended length. Also Gaussian approximation becomes increasingly inadequate with increasing crosslink density. For very short chains, for example $N \leq 5$, the mean chain extension in the unstrained state already exceeds that for which the Gaussian approximation is valid. Therefore non-Gaussian treatment is necessary for accurate determination of behavior even at smallest strains. Such a treatment is adopted by Kuhn [7] and he showed that the probability density *P(r)* is given by

$$\ln P(r) = const. - N\left[\frac{r}{nl}\beta + \ln\frac{\beta}{\sinh\beta}\right], \tag{33}$$

where $\beta = L^{-1}\left(\frac{r}{Nl}\right)$ is expressed in terms of Inverse Langevin function. This function is defined as:

$$L(\beta) = \coth\beta - 1/\beta\,. \tag{34}$$

The tension on a chain is derived in a manner similar to that of a Gaussian chain as

$$f = \frac{kT}{l}L^{-1}\left(\frac{r}{Nl}\right). \tag{35}$$

The complete force –extension relation is valid from *r/Nl* =0 to *r/Nl* =1, where the inverse Langevin function tends to infinity. In this work we will use the Non-Gaussian theory to characterize our network of polymer chains in the simulation. The Inverse Langevin function is approximated by the relation

$$L^{-1}(x) = x(3-x^2)/(1-x^2), \tag{36}$$

where x is any variable. Figure 5 shows the graph for Inverse Langevin and its approximation. The graph shows that as $x \to 1$ the function $L^{-1}(x) \to \infty$. This behavior is shown by the strain energy-strain curve of polymer model.

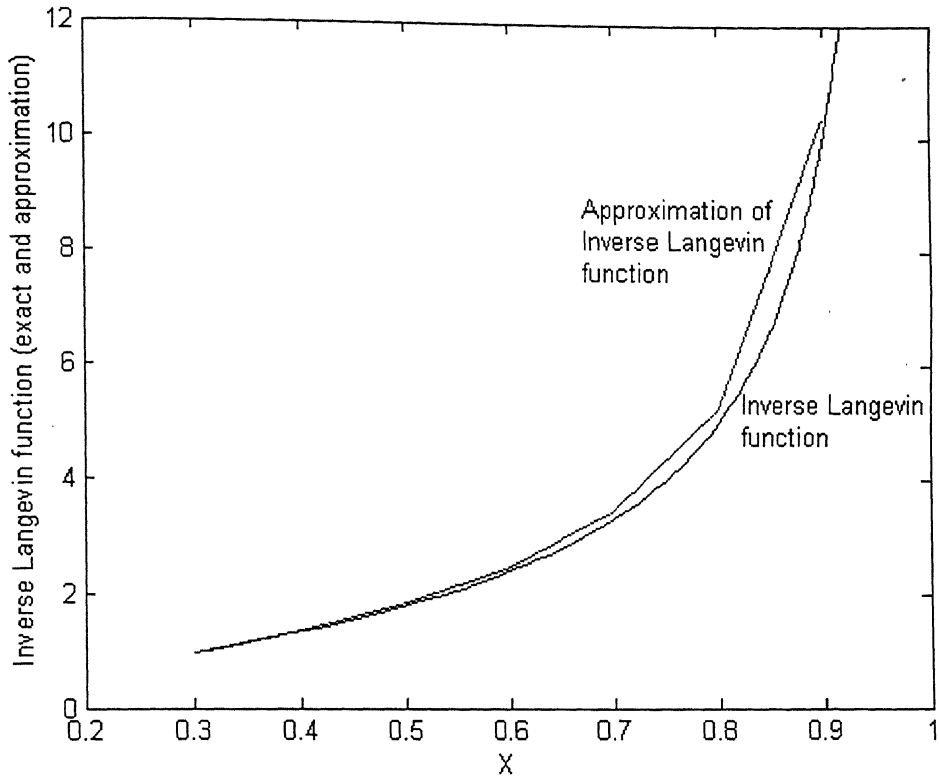

Figure 6 Inverse Langevin function exact and approximation

CHAPTER 3: SELF AVOIDING RANDOM WALK (S.A.W)

3.1 Introduction:

A polymer molecule can take many different shapes (conformations). This is due to its freedom of rotation about C-C bonds; for example ethane has two conformational states called eclipsed (energy maxima) state and staggered (energy minima) state as shown in Figure 1.

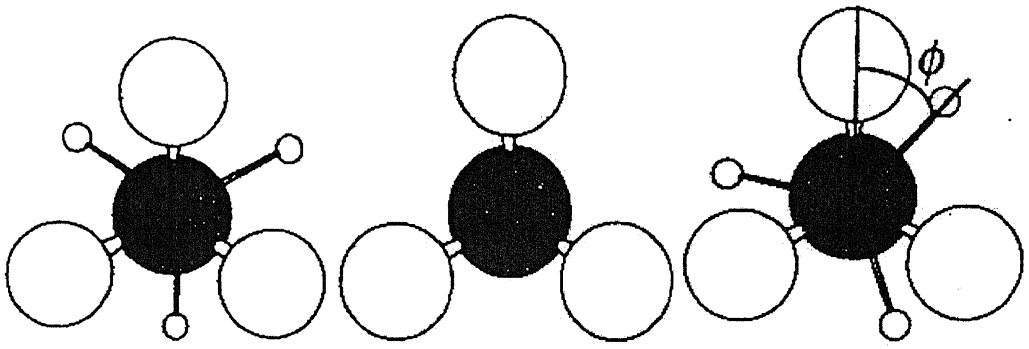

Staggered position (most stable) | Eclipsed position (least stable) | Intermediate position, definition of torsion angle(ϕ)

Figure 7 Rotational isomers of ethane from a view along the C-C bond: carbon-shaded; hydrogen-white

These conformation states are defined by the torsion angle ϕ between C-C bonds. Higher alkanes like n-butane have stable conformation states referred as trans(T) and gauche (G and G'). Higher alkanes exist in conformation states which are combination of these trans(T) and gauche(G and G') states. Flory developed Rotational Isomeric State Approximation method, which is a convenient way for dealing with conformational states of polymers. In this method each molecule is treated as existing only in state corresponding to potential energy minima, i.e. different combination of trans(T) and gauche(G and G') . Polymer chains exhibit in several cases a random (Gaussian) conformation, i.e. a random distribution of trans and gauche states. Random

macromolecular chains are found in solutions of polymers in good solvents, in polymer melts and also in glassy amorphous polymers.

An ensemble of polymer chains can only be described by means of spatial distribution functions. Two different measures of random chains are commonly used a) end-to-end distance(*r*) and b) radius of gyration (*s*). Former is distance between chain ends and latter is root-mean-square distance of collection of atoms from their center of gravity. Hence *s* is defined by

$$s^2 = \sum_{i=1}^{n} \frac{m_i \bar{r}_i^{\,2}}{r_i}. \qquad (1)$$

r_i is the vector from center of gravity to atom *I* of the polymer, m_i is the mass of i^{th} atom. For long chain polymers following Gaussian statistics the relation holds,

$$< s^2 >=< r^2 > /6. \qquad (2)$$

3.2 S.A.W: A sensible model for real polymers:

Real polymer molecules exist in continuous space having tetrahedral (109.47^0) bond angles, non trivial energy surface for bond rotational angles, and complicated monomer-monomer interaction potential, while S.A.W exist in discrete lattice with non-tetrahedral bond angles (e.g. 90^0 and 180^0 on simple cubic lattice), energy independent of bond rotational angles, and repulsive monomer-monomer potential. Inspite of these factors S.A.W is a perfect model for some aspects of behavior of linear polymers in good solvents (where the temperature of solvent is greater than theta solvents or solvents where coils expand). This behavior of S.A.W chain model arises from Universality, which plays a central role in modern theory of critical phenomenon. In short, critical statistical – mechanical systems are divided into small number of universality classes, which are typically characterized by spatial dimensionality, symmetries and other general properties. Near these critical points the leading asymptotic behavior is exactly same for all system of universality classes, details of chemical structure; interaction energies etc. are completely irrelevant. For this reason it is essential to determine universal and non-universal quantities.

To determine universal quantities, any mathematical model belonging to the same universality class as the system under study is taken, and solving it to determine the exact values of universal quantities.

The behavior of polymer molecule as the chain length tends to infinity is a critical phenomenon in above sense. It is found that mean-square radius of gyration $< s^2 >$ of linear polymer molecule consists of N monomers units has leading asymptotic behavior,

$$< s^2 >= AN^{2\nu} f(N) . \qquad (3)$$

Here $f(N)$ is some function of N; as $N \to \infty$ where critical exponent $\nu \approx 0.588$ is universal, i.e. exactly the same for all polymers, solvents and temperature (temperature greater than theta temperature). The critical amplitude A is non-universal, i.e. it depends on the polymer solvent and temperature. Therefore linear polymer chains which exhibit some flexibility and has short range predominantly repulsive monomer-monomer interaction lies in the same universal class as that of S.A.W.

3.3 S.A.W: notation and terms.

Let L be some regular d-dimension lattice. A N-step (S.A.W) ω on L is a sequence of distant point $\omega_0, \omega_1, ...\omega_N$ in L such that each point is the nearest neighbor of its predecessor. N is the number of steps in ω. Following are the measuring terms of the size of N-step S.A.W.

- The squared end-to-end distance of S.A.W.

$$r^2 = (\omega_n - \omega_0)^2 . \qquad (4)$$

- The squared radius of gyration

$$s = \frac{1}{2(N+1)^2} \sum_{i,j}^{N} (\omega_i - \omega_j)^2 . \qquad (5)$$

- The mean-square distance of a monomer from the endpoint

$$r_m^2 = \frac{1}{2(N+1)} \sum_{i=0}^{N} \left[(\omega_i - \omega_0)^2 + (\omega_i - \omega_N)^2 \right] . \qquad (6)$$

The mean values $< r^2 >_N, < s^2 >_N$ *and* $< r_m^2 >_N$ are believed to have asymptotic behavior

$$< r^2 >_N, < s^2 >_N, < r_m^2 >_N \sim N^{2\nu}$$

as $N \to \infty$,where ν is another (universal) critical exponent. Moreover the amplitude ratios;

$$A_N = \frac{< s^2 >_N}{< r^2 >_N}, \tag{7a}$$

$$B_N = \frac{< r_m^2 >_N}{< r^2 >_N}. \tag{7b}$$

are expected to approach universal values in the limit $N \to \infty$.

3.4 Generation of the model of polymer solid:

3.4.1 Introduction:

The fundamental concept of rubber elasticity put forward by Meyer, von Susich and Volko [4] developed the relation between elasticity and the ability of the chain to take up an irregular or statistically determined form by virtue of the interchange of energy between its constituent elements and surrounding atoms. Later on Karrer [4] noted the properties of long chain structures and found that in long chain molecules in which internal rotation about bonds can take place will be subjected to Brownian motion at various portions of its structure. This so-called micro-Brownian motion of the individual elements of long chain molecules is similar to the thermal motion of molecules of an ordinary liquid, with the single difference that the moving units, instead of being entirely independent, are connected together in form of chain. It is known that properties of the forces exerted by one molecule on another (secondary forces which are weak Van der Waals forces) are of the same order of magnitude as the intermolecular forces in an ordinary low-molecular weight liquid. These Van der Waals forces are necessary if the random rotations and the resulting changes in configuration of the molecules upon which their elasticity depends are to take place.

3.4.2 Model Generation:

The undeformed polymer solid is represented by a dense network of coiled, entangled macromolecules as shown in Figure 2. We start with a regular array of entanglement points depicted in Figure 3. Entanglement points are topologically defined points in

polymer model through which a polymer molecular chain passes when it is in motion. The chain segments between entanglements are tied together by Van der Waals force or bonds (dotted lines). These secondary forces provide the necessary initial stiffness to the material. For convenience the three-dimensional network is given a planar conformation.

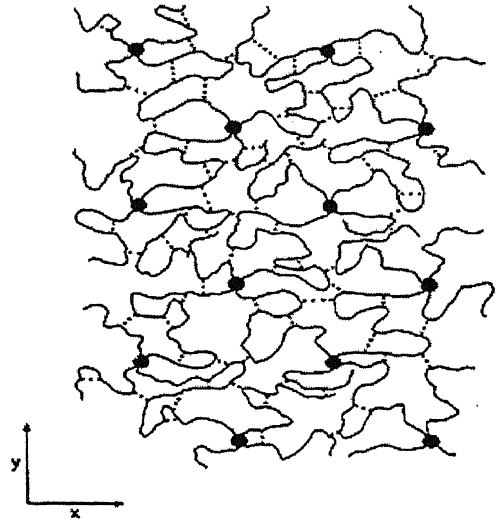

Figure 8 Schematic representation of the undeformed polymer solid

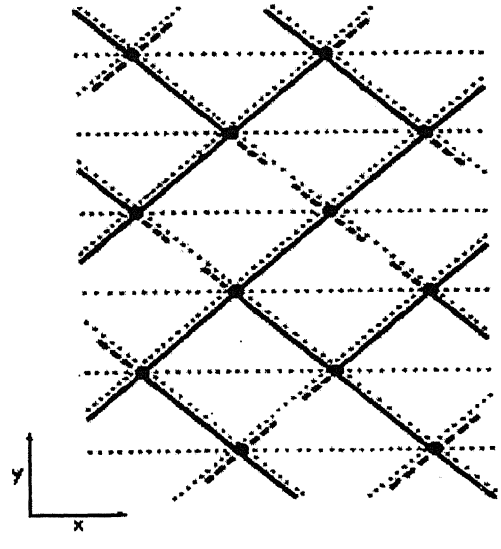

Figure 9 A more schematic representation of the network, in which the details of chain configuration are omitted altogether

Van der Waals bonds are represented by dotted lines and solid lines denote chain vectors between entanglements. In three dimensional space chain vectors are randomly oriented in an actual, undeformed specimen i.e. $< \cos^2 \theta >= 1/3$, where θ is the vector angle with the draw axis. In the two–dimensional representation we take the same angle as $\theta = 54.7^{o}$ for all vector orientation along the y-axis.

3.4.3 S.A.W representation of a single chain:

A single chain is represented by S.A.W; the algorithm used for generation of S.A.W is as follows (in our algorithm we start the chain from first entanglement point of the regular grid):

Title: S.A.W single chain

Subroutine: SC (N)

Comment: This subroutine returns S.A.W chain

$\omega \leftarrow [\omega_0]$

start: **for i=1 to N do**

$\omega_i \leftarrow$ **a random nearest neighbor of** ω_{i-1}

if $\omega_i \in \{\omega\}$

$\omega_i = \omega_{i-1}$

goto start

else

$\omega_{i-1} = \omega_i$

end do.

Here ω is the sequence of distant points $\omega_0, \omega_1, \ldots\ldots \omega_N$ where each member is the nearest neighbor of its predecessor, N is the number of steps of S.A.W (chain), ω_0 is he start point of the chain. S.A.W of 100 steps generated by using this algorithm is shown below in Figure 4.

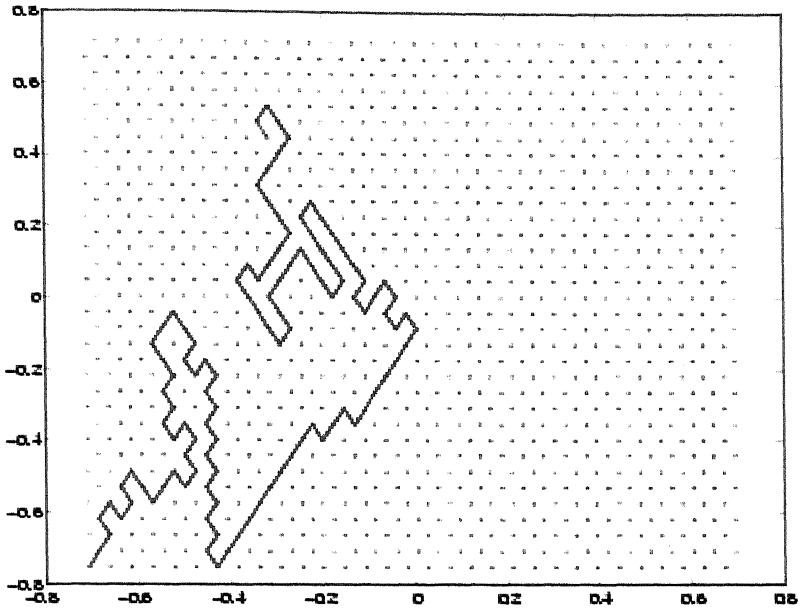

Figure 1 Single chain generated using S.A.W

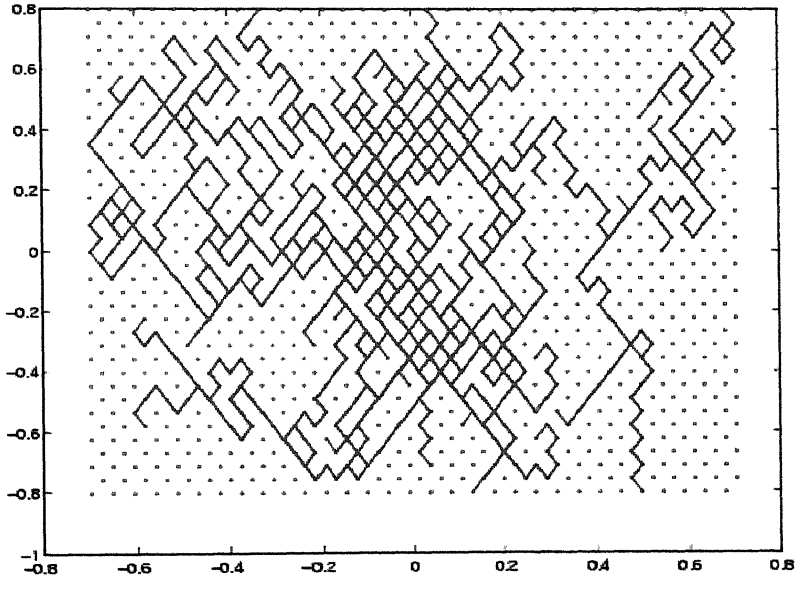

Figure 2 Multiple chains generated

3.4.4 Multiple chains generation:

Multiple chains are generated by using the algorithm shown below:

Title: Multiple Chain

function: MC(ω)

Comment: this routine returns multiple S.A.W chains

start: call subroutine SC(N)

if

present node and the node to which the chain is to move is in some previous chain then move to the nearest neighbor of present node which is not in any of the previous chains.
end if.

This algorithm takes care of the restriction on the chains that they should not overlap other chains. For modeling of polymer this restriction is required because no two chain strands can occupy the same position in space due to repulsion of the bonds. See Figure 5

3.4.5 Applying boundary conditions to the polymer model:

We had considered the polymer model to be taken out of a large polymer specimen which is continuous in x-direction and so we had applied periodic boundary condition in x-direction. However we have chopped the chains which are going out of the grid from extreme y-coordinates (See Figure 6).

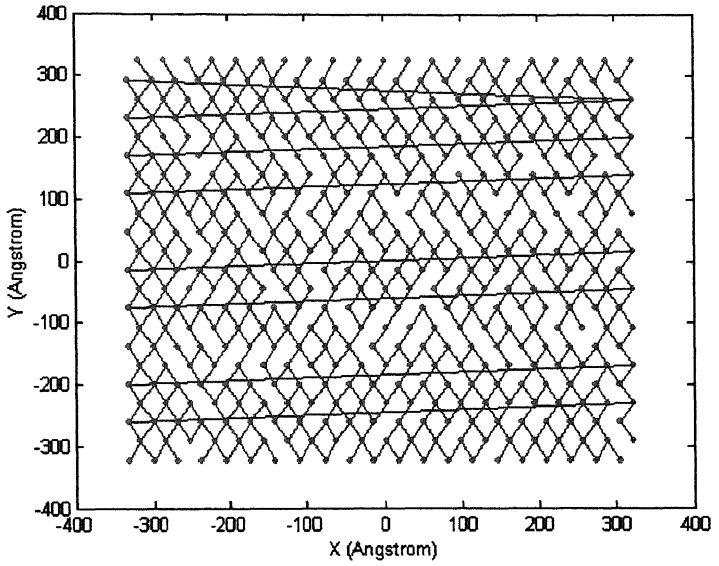

Figure 3 Multiple chains showing periodic boundary conditions applied to the model

From the Figure it can be seen that the lines between nodes at extreme x-coordinates of the grid depicts the continuity of the grid patch in x-direction.

3.4.6 Final model:

Final model of the polymer is obtained by taking into consideration both Van der Waals bonds and the primary bonds which are due to C-C bonds. Here it is worth mentioning that the chain segments between two entanglement points (we call them strands) are made up of large number of atoms which constitute the polymer molecule. See Figure 6. In the figure the red lines show the Van der Waals bonds and the blue lines show the molecular chain obtained from S.A.W algorithm.

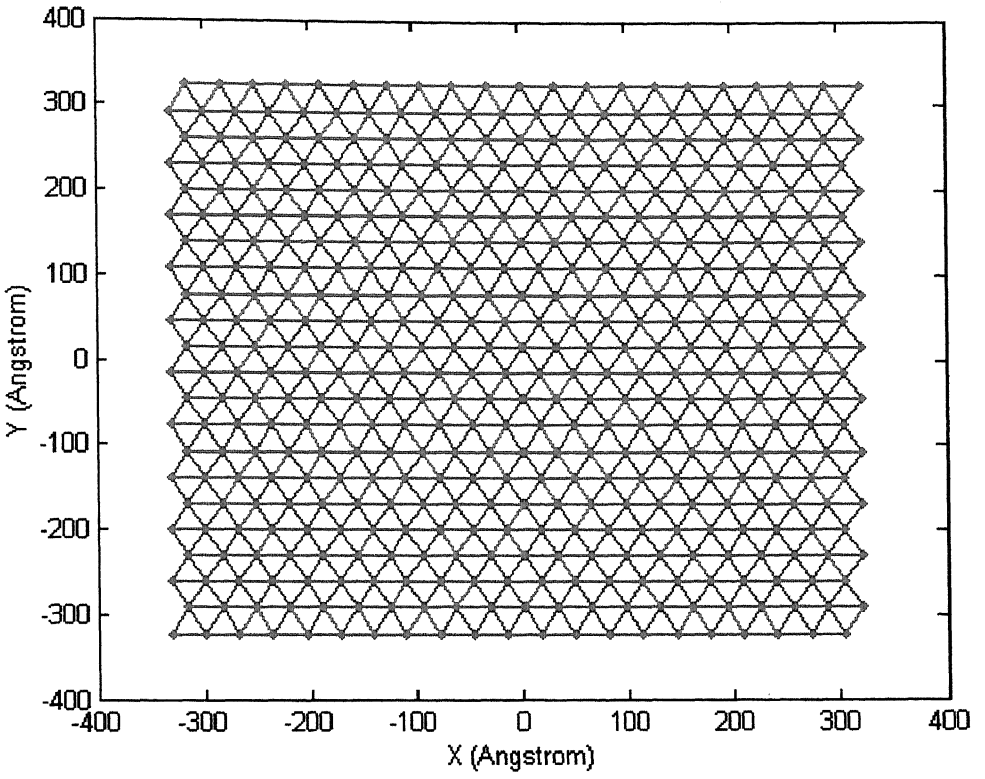

Figure 4 Final model of the polymer with Van der Waals bond and molecular bonds present

CHAPTER 4: SIMULATING SAW MODEL

4.1Introduction:

The model of polymer developed using S.A.W is like a truss structure, each element of this structure is like a spring that experiences large deformations and rotation, and the stress-strain relation of this element is also nonlinear, this give rise to geometric nonlinearity and material nonlinearity respectively. Hence when we analyzed the model using Finite Element Methods geometric nonlinearity and material nonlinearity were implemented in the analysis methods of the model.

4.2 Finite Element Formulation:

The S.A.W model is analyzed using corotational Lagrangian meshes [17] where the nodes and elements move with the material. Boundaries and interfaces treatment is simplified as they remain coincident with element edges. Lagrangian meshes are advantageous for history-dependent materials because in Lagrangian formulation constitutive equations are always evaluated at the same material points.

Finite element discretisation with Lagrangian meshes are classified as

1) Updated Lagrangian Formulation and
2) Total Lagrangian Formulation.

Here both formulations use Lagrangian description, i.e. dependent variables are function of material (Lagrangian) coordinate and time. We are using total Lagrangian formulation, where the weak form involves integrals over the initial (reference) configuration and the derivatives are taken with respect to material coordinate.

In Total Lagrangian Formulation Green strain tensor is used as a measure of strain and corresponding stress is Second Piola-Kirchoff stress (PK2) but we will use nominal stress also where required, the reason for this will be explained latter. A weak form of momentum equation is developed, which is known as principle of virtual work.

4.2.1 Some terms and designation:

D is the deformation in terms of velocity or displacement; velocity is denoted by $\mathbf{v}(\mathbf{X},t)$, Cauchy stress is denoted by $\sigma(\mathbf{X},t)$, rate of deformation is denoted by $\mathbf{D}(X,t)$ and density is denoted by $\rho(\mathbf{X},t)$,all these variable are dependent variables. Nodal coordinates in current configuration are denoted by x_{iI}, $I=1$ to n (n is the number of nodes). Lower case subscript are used for component, upper case subscript are for nodal values. Nodal coordinates in deformed configuration are X_{iI}.

In finite element method, motion $\mathbf{x}(\mathbf{X},t)$ is approximated by the relation

$$\mathbf{x}(\mathbf{X},t)=\mathbf{N}_I(\mathbf{X})x_{iI}(t) \text{ or } \mathbf{x}(\mathbf{X},t)=\mathbf{N}_I(\mathbf{X})\mathbf{x}_I(t). \tag{1}$$

Where $N_I(X)$ is the interpolation (shape) function and x_I is the position vector of node I.

We define the nodal displacement at the nodes by

$$u_{iI}(t)=x_{iI}(t)-X_{iI} \text{ or } u_I(t)=x_I(t)-X_I. \tag{2}$$

The velocities are obtained by taking the material time derivative of the displacement, given by

$$v_i(X,t)=\frac{\partial u_i(X,t)}{\partial t}=\dot{u}_{iI}(t)N_I(X) \text{ or } v(X,t)=\dot{u}_i(t)N_I(X). \tag{3}$$

f_{iI}^{int} and f_{iI}^{ext} are the internal and external nodal forces. Define matrix ***B*** as

$$B_{jI}=\frac{\partial N_I}{\partial x_j} \text{ or } \mathbf{B}=\left[B_{jI}\right]=\left[\frac{\partial N_I}{\partial x_j}\right]. \tag{4}$$

4.2.2 Corotational Formulation:

In structural elements such as bars, beams and shells fixed coordinate systems makes the analysis of structure difficult, for example a rotating rod. Initially σ_x is the only non-zero stress and σ_y vanishes, as the rod rotates its become awkward to express state of uniaxial stress in terms of global component of stress tensor. To overcome this difficulty coordinate system is embedded in the bar and is rotated with the rod, this is the concept

of corotational formulation and the coordinate system is known as corotational coordinate. This concept of corotational formulation is used in our F.E.A.

4.2.3 Total Lagrangian Formulation:

Governing Equations:

In Total Lagrangian Formulation nominal stress $\boldsymbol{P}$ is used in momentum equation because the resulting momentum equation and its weak form are simpler than that for PK2 stress. PK2 stress is used in constitutive equation as $\boldsymbol{P}$ is not symmetric. Deformation tensor $\boldsymbol{F}$ does not vanish in rigid body rotation hence is not suitable for measuring strain in constitutive equation and constitutive equation is written in terms of Green strain tensor $\boldsymbol{E}$. Consider a mass with domain Ω and boundary defined by Γ, as shown in Figure1.

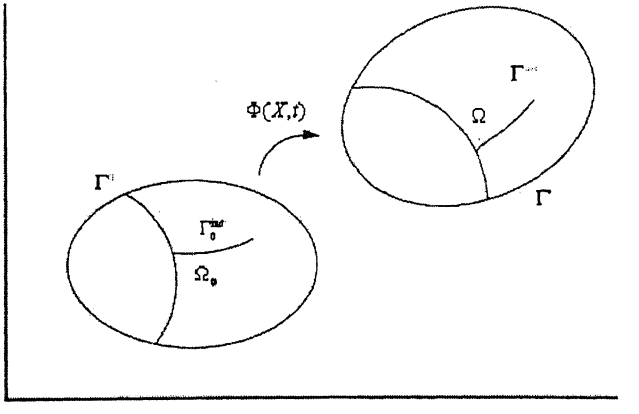

Figure 14 Deformed and undeformed body

Governing equations for Total Lagrangian formulation are as follows (subscript '0' signifies variable with respect to undeformed position, while 'int', 'ext' and 'kin' superscripts denote internal, external and inertial values of the variables):

Conservation of mass:

$$\rho J = \rho_0 J_0 = \rho_0 . \tag{5}$$

Here ρ is the density and J is the determinant of Jacobian between spatial and material coordinates.

Conservation of linear momentum:

$$\nabla_0 \cdot \mathbf{P} + \rho_0 \mathbf{b} = \rho_0 \ddot{\mathbf{u}}. \tag{6}$$

Here ***b*** is the body force.

Conservation of angular momentum:

$$\mathbf{F} \cdot \mathbf{P} = \mathbf{P}^T \cdot \mathbf{F}^T. \tag{7}$$

Conservation of energy:

$$\rho_0 \dot{w}^{\text{int}} = \dot{\mathbf{F}}^T : \mathbf{P} - \nabla_0 \cdot \bar{\mathbf{q}} + \rho_0 s. \tag{8}$$

$\dot{w}^{\text{int}}$ is the rate of internal work done, q is heat flux, s is the power supplied by heat sources, here $\bar{\mathbf{q}} = J\mathbf{F}^{-1} \cdot \mathbf{q}$.

Constitutive equation:

$$\boldsymbol{S}=\boldsymbol{S}\ (\boldsymbol{E}...etc.),\ \mathbf{P} = \mathbf{S} \cdot \mathbf{F}^T. \tag{9}$$

Here **S** is PK2.

Measure of strain:

$$\mathbf{E} = \frac{1}{2}(\mathbf{F}^T \cdot \mathbf{F} - \mathbf{I}). \tag{10}$$

I is identity matrix.

Boundary conditions:

$$n_j^0 P_{ji} = \bar{t}_i^0 \ or\ \mathbf{e}_i \cdot \mathbf{n}^0 \cdot \mathbf{P} = \mathbf{e}_i \cdot \bar{\mathbf{t}}_0 \ on\ \Gamma_{ti}^0, \tag{11}$$

Here n is the unit normal, t is the surface traction, e_i is the base vectors of coordinates.

$$u_i = \bar{u}_i \ on \Gamma_{u_i}^0, \qquad \Gamma_{t_i}^0 \cup \Gamma_{u_i}^0 = \Gamma^0, \quad \Gamma_{t_i}^0 \cap \Gamma_{u_i}^0 = 0, \quad \text{for i=1 to } n_{sd} \tag{12}$$

where n_{sd} is the number of space dimensions.

Initial conditions:

$$\mathbf{P}(\mathbf{X},0)=\mathbf{P}_0(\mathbf{X})\,. \tag{13}$$

$$\dot{\mathbf{u}}(\mathbf{X},0)=\dot{\mathbf{u}}_0(\mathbf{X})\,. \tag{14}$$

Internal continuity condition:

$$n_j^0 P_{ji}=0 \ on\ \Gamma_{\text{int}}^0\,. \tag{15}$$

4.2.4 Total Lagrangian Weak Form:

We will develop weak form from strong form. Here the strong form consists of momentum equation (6), traction boundary conditions (12) and internal continuity condition (15). Defining spaces for test and trail functions as

$$\delta\mathbf{u}(X)\in U_0,\ \mathbf{u}(X,t)\in U \tag{16}$$

U is the space of kinematically admissible displacements U_0 is the same space with the additional requirement that the displacements vanish on displacement boundaries.

To develop weak form momentum equation is multiplied by test function and is integrated over the initial configuration and we get

$$\int_{\Omega_0}\delta u_i\left(\frac{\partial P_{ji}}{\partial X_j}+\rho_0 b_i-\rho_0\ddot{u}_i\right)d\Omega_0=0\,. \tag{17}$$

Finally we get weak form as

$$\delta w^{\text{int}}(\delta\mathbf{u},\mathbf{u})-\delta w^{ext}(\delta\mathbf{u},\mathbf{u})+\delta w^{kin}(\delta\mathbf{u},\mathbf{u})=0\quad\forall\delta\mathbf{u}\in U_0\,. \tag{18}$$

Here we have

$$\delta w^{\text{int}}=\int_{\Omega_0}\delta\mathbf{F}^T:\mathbf{P}d\Omega_0\,. \tag{19}$$

$$\delta w^{ext}=\int_{\Omega_0}\delta u_i\rho_0 b_i d\Omega_0+\sum_{i=1}^{n_{stl}}\int_{\Gamma_{t_i}^0}\delta u_i\,\bar{t}_i^0\,. \tag{20}$$

$$\delta w^{kin}=\int_{\Omega_0}\delta\mathbf{u}\cdot\rho_0\ddot{\mathbf{u}}\,d\Omega_0\,. \tag{21}$$

From weak form (17) it is clear that work done due to internal force is equal to sum of work done by external force and inertial force, hence for finite element analysis of the model we can just obtain the value of internal force.

Internal nodal force:

From (19) $\delta w^{\text{int}} = \int_{\Omega_0} \delta F_{ji} P_{ji} d\Omega_0 = \delta u_{iI} \int_{\Omega_0} \frac{\partial N_I}{\partial X_j} P_{ji} d\Omega_0$. (22)

From (4) and (22)

$$\mathbf{f}_{iI}^{\text{int}} = \int_{\Omega_0} \mathbf{B}_0^T \mathbf{P} d\Omega_0 \,. \tag{23}$$

4.2.5 Linearization:

Linearization of internal nodal forces is done and we derive the tangent stiffness matrix K^{int} for Lagrangian elements. Linearization of the constitutive equation is carried out with the continuum tangent moduli, the resulting material tangent stiffness matrix is called the tangent stiffness matrix. The tangent stiffness matrix is expressed in terms of C^{SE}, the tangent moduli relating the rate of PK2 stress to rate of Green strain in the total Lagrangian framework. Tangent stiffness matrix is developed by relating the rates of the internal nodal forces f^{int} to the nodal velocities $\dot{d}$. Taking the material time derivative of (23) we get

$$\dot{\mathbf{f}}^{\text{int}} = \int_{\Omega_0} \mathbf{B}_0^T \dot{\mathbf{P}} d\Omega_0 \; or \; \dot{\mathbf{f}}_{iI}^{\text{int}} = \int_{\Omega_0} \frac{\partial N_I}{\partial X_j} \dot{P}_{ji} d\Omega_0 . \tag{24}$$

To obtain the stiffness matrix K^{int} strain rate $\dot{P}$ is expressed in nodal velocities using the constitutive equation and the strain measure, here we use material time derivative of the PK2 stress. Time derivative of the transformation $P = S \cdot F^T$ is given by

$$\dot{\mathbf{P}} = \dot{\mathbf{S}} \cdot \mathbf{F}^T + \mathbf{S} \cdot \dot{\mathbf{F}}^T \; or \; \dot{P}_{ij} = \dot{S}_{ir} \cdot F_{rj}^T + S_{ir} \dot{F}_{rj}^T \,. \tag{25}$$

from (24) and (25)

$$\dot{f}_{il}^{\text{int}} = \int_{\Omega_0} \frac{\partial N_I}{\partial X_j}(\dot{S}_{jr} \cdot F_{ir} + S_{jr}\dot{F}_{ir})d\Omega_0 \quad \text{or} \quad df_{il}^{\text{int}} = \int_{\Omega_0} \frac{\partial N_I}{\partial X_j}(dS_{jr} \cdot F_{jr} + S_{jr}\, dF_{ir})d\Omega_0 \ .$$

(26)

From (26) it is evident that the rate of internal nodal forces consists of two parts:

1) The first part which involves the rate of stress ($\dot{S}$) depends upon material response and leads to material stiffness matrix denoted by K^{mat}.

2) The second part involves the current state of stress S, and leads to geometric effects of deformation (including rotation and stretching). This term is called geometric stiffness and is denoted by K^{geo}.

The internal nodal force can now be written as:

$$\dot{\mathbf{f}}^{\text{int}} = \dot{\mathbf{f}}^{mat} + \dot{\mathbf{f}}^{geo} \quad or \quad \dot{f}_{il}^{\text{int}} = \dot{f}_{il}^{mat} + \dot{f}_{il}^{geo} \ . \tag{27}$$

First term in (27) material rate of internal nodal forces and second term is geometric rate of internal nodal forces.

Material tangent stiffness:

Voigt form of notation is convenient in developing tangent stiffness matrix as the tensor of tangent moduli C_{ijkl} is forth order tensor and cannot be handled readily by standard matrix operation. From equation (26) and (27) we get

$$\dot{\mathbf{f}}^{mat} = \int_{\Omega_0} \mathbf{B}_0^T \{\dot{\mathbf{S}}\} d\Omega_0 \tag{30}$$

where $\{\dot{S}\}$ is rate of Pk2 stress in Voigt column matrix form. Now constitutive equation is written as

$$\dot{S}_{ij} = C_{ijkl}^{SE} \dot{E}_{kl} \qquad \text{or} \quad \{\dot{S}\} = [C^{SE}]\{\dot{E}\} \tag{31}$$

and the rate of the Green strain to nodal velocities in Voigt notation is given by $\{\dot{\mathbf{E}}\} = \mathbf{B}_0 \dot{d}$. From (30) and (31) we get

$$\dot{\mathbf{f}}^{\text{int}}_{mat} = \int_{\Omega_0} \mathbf{B}_0^T \left[\mathbf{C}^{SE}\right] \mathbf{B}_0 d\Omega \dot{d} . \tag{32}$$

Finally the material stiffness matrix is obtained as

$$\mathbf{K}^{mat} = \int_{\Omega_0} \mathbf{B}_0^T \left[\mathbf{C}^{SE}\right] \mathbf{B}_0 d\Omega_0 \quad or \quad \mathbf{K}_{IJ}^{mat} = \int_{\Omega_0} \mathbf{B}_{0I}^T \left[\mathbf{C}^{SE}\right] \mathbf{B}_{0J} d\Omega_0 . \tag{33}$$

Geometric stiffness:

The geometric stiffness is obtained from relation $B_{iI}^0 = \partial N_I / \partial X_i$ and from (26) and (27)

$$\mathbf{K}_{IJ}^{geo} = \mathbf{I} \int_{\Omega_0} \mathbf{B}_{0I}^T \mathbf{S} \mathbf{B}_{0J} d\Omega_0 . \tag{34}$$

From (34) we see that PK2 stress is in the form of tensor, i.e. a square matrix. Each submatrix of the geometric stiffness matrix is unit matrix, hence the geometric stiffness matrix is invariant with rotation, i.e. $\hat{\mathbf{K}}_{IJ}^{geo} = \mathbf{K}_{IJ}^{geo}$, here the superposed denotes the geometric stiffness matrix on rotated coordinate system (corotational form).

Material and geometric tangent stiffness matrix for an element:

To obtain the material and geometric stiffness matrix for an element consider the element as a two-node rod element in two dimensions as shown in the Figure 2. The element is in uniaxial state of stress with the only non-zero stress along the axis of bar. To simplify the formulation, consider material coordinate system to coincide with the axis of the rod (Corotational formulation), with the origin of the material coordinate at node 1. The parent material coordinate is $\xi \in [0,1]$. The material coordinate is related to the element coordinates by

$$X = X_2 \xi = l_0 \xi . \tag{35}$$

Here l_0 is the initial length of the element. The motion is given in terms of the element coordinates by

$$\begin{Bmatrix} x \\ y \end{Bmatrix} = \begin{bmatrix} x_1 & x_2 \\ y_1 & y_2 \end{bmatrix} \begin{Bmatrix} 1-\xi \\ \xi \end{Bmatrix} \quad \text{or} \quad \mathbf{x}(\xi, t) = \mathbf{x}_I(t) \mathbf{N}_I(\xi) . \tag{36}$$

where

$$\{N_I(\xi)\}^T = \begin{bmatrix}(1-\xi) & \xi\end{bmatrix} = \begin{bmatrix}1-\frac{X}{l_0} & \frac{X}{l_0}\end{bmatrix}. \tag{37}$$

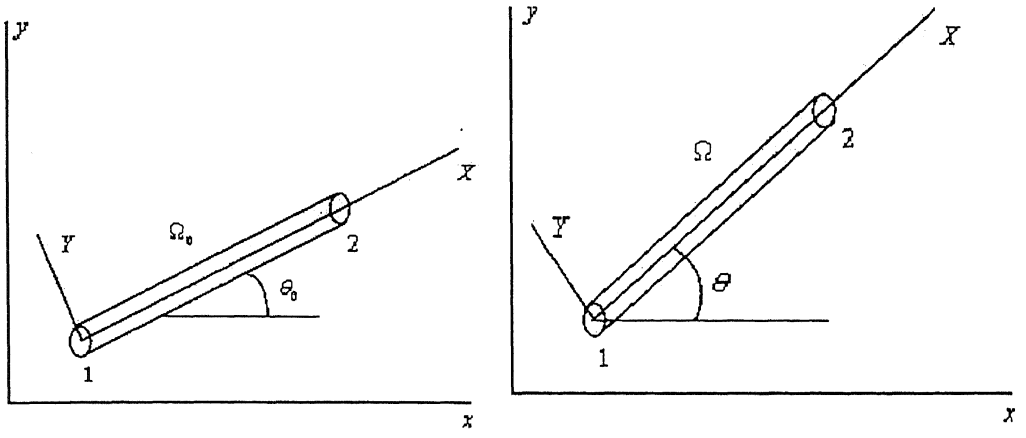

Initial Current

Figure 15 Rod element in two dimensions in total Lagrangian formulation

The $\mathbf{B}_0$ matrix from (4) is defined as

$$[B_{0iI}] \equiv [\partial N_I / \partial X_i]^T = \frac{1}{l_0}[-1 \quad +1]. \tag{38}$$

Let us take the coordinates of node 1 and node 2 as $[x_1 \quad y_1]^T$ and $[x_2 \quad y_2]^T$ respectively.

Define $x_{21} = x_2 - x_1$ and $y_{21} = y_2 - y_1$, hence we can get $\cos\theta = x_{21}/l$ and $\sin\theta = y_{21}/l$.

Here 'l' is the deformed length of the element. In corotational formulation the only non-zero stress is along the axis of the rod. The X axis coincides with the axis of the rod, so S_{11} is always the stress component along the axis of the rod and in Voigt notation only the first row of the $\mathbf{B}_0$ matrix need to be considered. The $\mathbf{B}_I^0$ matrix is written as in Voigt notation as:

$$\mathbf{B}_I^0 = \begin{bmatrix} \dfrac{\partial N_I}{\partial X}\dfrac{\partial x}{\partial X} & \dfrac{\partial N_I}{\partial X}\dfrac{\partial y}{\partial X} \\ \dfrac{\partial N_I}{\partial Y}\dfrac{\partial x}{\partial Y} & \dfrac{\partial N_I}{\partial Y}\dfrac{\partial y}{\partial Y} \\ \dfrac{\partial N_I}{\partial X}\dfrac{\partial x}{\partial Y}+\dfrac{\partial N_I}{\partial Y}\dfrac{\partial x}{\partial X} & \dfrac{\partial N_I}{\partial X}\dfrac{\partial y}{\partial Y}+\dfrac{\partial N_I}{\partial Y}\dfrac{\partial y}{\partial X} \end{bmatrix}. \tag{39}$$

Now we have $x,X = x_{21}/l_0 = l/l_0 \cos\theta$, $y,X = y_{21}/l_0 = l/l_0 \sin\theta$. The first row of the $\mathbf{B}_0$ from (39) is given by

$$\mathbf{B}_I^0 = \begin{bmatrix} N_{I,X}\, x_{,X} & N_{I,X}\, y_{,X} \end{bmatrix} = \begin{bmatrix} N_{I,X}\, x_{21} & N_{I,X}\, y_{21} \end{bmatrix}. \tag{40}$$

From (37) we have

$$\mathbf{B}_0 = \begin{bmatrix} \mathbf{B}_1^0 & \mathbf{B}_2^0 \end{bmatrix} = \frac{l}{l_0^2}\begin{bmatrix} -\cos\theta & -\sin\theta & \cos\theta & \sin\theta \end{bmatrix}. \tag{41}$$

Material tangent stiffness matrix:

From (33) and (41) we get

$$\mathbf{K}^{mat} = \frac{A_0 C^{SE}}{l_0}\left(\frac{l}{l_0}\right)^2 \begin{bmatrix} \cos^2\theta & \cos\theta\sin\theta & -\cos^2\theta & -\cos\theta\sin\theta \\ & \sin^2\theta & -\cos\theta\sin\theta & -\sin^2\theta \\ & & \cos^2\theta & \cos\theta\sin\theta \\ \textit{symmetric} & & & \sin^2\theta \end{bmatrix}. \tag{42}$$

Here A_0 is the undeformed cross section area of the rod element.

Geometric tangent stiffness matrix:

From (34) and (38) we get

$$\mathbf{K}^{geo} = \frac{A_0 S_{11}}{l_0}\begin{bmatrix} +1 & 0 & -1 & 0 \\ 0 & +1 & 0 & -1 \\ -1 & 0 & +1 & 0 \\ 0 & -1 & 0 & +1 \end{bmatrix}. \tag{43}$$

(42) and (43) holds for any orientation of the element and the total tangent stiffness matrix is the sum of the material and geometric stiffness.

In Updated Lagrangian form material and geometric stiffness matrix can be written as

$$\mathbf{K}^{mat} = \frac{AE^{\sigma\tau}}{l}\begin{bmatrix} \cos^2\theta & \cos\theta\sin\theta & -\cos^2\theta & -\cos\theta\sin\theta \\ & \sin^2\theta & -\cos\theta\sin\theta & -\sin^2\theta \\ & & \cos^2\theta & \cos\theta\sin\theta \\ \textit{symmetric} & & & \sin^2\theta \end{bmatrix}. \tag{44}$$

and

$$\mathbf{K}^{geo} = \frac{A\sigma_{xx}}{l}\begin{bmatrix} +1 & 0 & -1 & 0 \\ 0 & +1 & 0 & -1 \\ -1 & 0 & +1 & 0 \\ 0 & -1 & 0 & +1 \end{bmatrix}. \tag{45}$$

$E^{\sigma\tau}$ is the tangent moduli relating the Truesdell rate of the Cauchy stress to the rate-of deformation in the updated Lagrangian formulation. σ_{xx} is the only Cauchy stress present.

According to classical theory of rubber elasticity for non-Gaussian chain force on a chain strand having a vector length r is given by [4]

$$f = \frac{kT}{l_s} L^{-1}\left(\frac{r}{Nl_s}\right). \tag{46}$$

Where N is the number of statistical chain segments l_s is there length. L^{-1} is the inverse Langevin function. Now stiffness of this strand K_S is obtained from $\partial f / \partial r$ using the approximation for Langevin function

$$L^{-1}(s) = s(3-s^2)/1-s^2 \quad (s \text{ is any variable})$$

as

$$K_s = \frac{3N^5 l_s^5 + Nl_s r^4}{(N^3 l_s^3 - Nl_s r^2)^2} \tag{47}$$

Also there is Van der Waals force present in the model and the force for particular Van der Waals element is obtained as

$$f_{vd} = K\varepsilon / \alpha \tag{48}$$

where f_{vd} is the force in the Van der Waals element, K is the stiffness and ε is the strain in the Van der Waals element. Following [4]

$$\alpha = (n/3)N^{1/2}. \tag{49}$$

Final stiffness of an element is due to both strand stiffness and also Van der Waals stiffness. Hence (45) and (46) becomes

$$\mathbf{K}^{mat} = \frac{K_s + K}{l}\begin{bmatrix} \cos^2\theta & \cos\theta\sin\theta & -\cos^2\theta & -\cos\theta\sin\theta \\ & \sin^2\theta & -\cos\theta\sin\theta & -\sin^2\theta \\ & & \cos^2\theta & \cos\theta\sin\theta \\ symmetric & & & \sin^2\theta \end{bmatrix}. \tag{50}$$

and

$$\mathbf{K}^{geo} = \frac{f + f_{vd}}{l}\begin{bmatrix} +1 & 0 & -1 & 0 \\ 0 & +1 & 0 & -1 \\ -1 & 0 & +1 & 0 \\ 0 & -1 & 0 & +1 \end{bmatrix}. \tag{51}$$

We can now analyze the model of the polymer using (50) and (51) to get the strain energy vs. strain and stress vs. strain curves.

CHAPTER 5: RESULTS AND DISCUSSION

5.1 Introduction and objective of the study:

Polymer model developed in chapter 3 was used and the results obtained from these analyses were used to predict the mechanical behavior of amorphous polymers. The purpose of this work is to demonstrate that the model based on rubber elasticity has the potential of qualitatively and quantitatively predicting the properties of amorphous, glassy polymers.

5.2 Actual stress-strain curve of an amorphous polymer:

Figure 1 shows that there are three distinct regions on the true stress-strain response of a polymer.

1) Initially the stress rises in an approximately linear manner as the applied strain increases. In this region the load bearing capacity of the polymer derives from both Van der Waals as well as molecular bonds in chain strands.
2) At the yield point there is a abrupt fall in true stress. The fall in true stress is due to breakage to Van der Waals bonds which are weaker than strands and break earlier than strands.

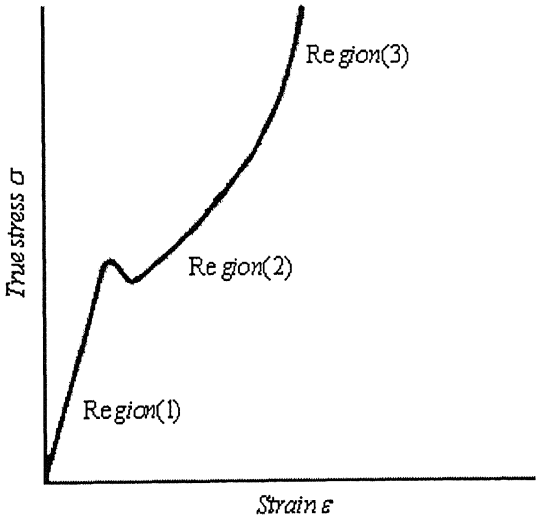

Figure 16 Actual Stress-Strain curve of a polymer showing different stages of deformation

After breakage of Van der Waals bonds the entire load is taken by the strands.

3) Finally at large extensions the slope of the stress-strain curve increases again, i.e. a strain hardening effect occurs. This is because chains orient in the direction of stretch.

5.3 Defining the problem:

We had taken a regular grid of five hundred nodes (entanglement points) with periodic boundary conditions applied in x-direction. Polymer chains were obtained on this grid using S.A.W. Each strand is taken as a finite element in our model. Later on Van der Waals forces are applied between all nodes which add up to the stiffness of the model.

5.3.1 Application of boundary conditions:

Displacement boundary conditions are applied to the specimen in the y-direction. The nodes at the top of the specimen are given a displacement in the y-direction and the nodes at the bottom of the specimen are fixed and cannot move in y-direction. However, they are free to move in x-direction. The nodes at the extreme left of the grid are fixed in x-direction and the nodes at the extreme right of the grid are given a displacement in x-direction, so that the volume of the specimen remains constant. We had taken λ as the stretch of specimen in the y-direction, as the two-dimensional model system is assumed to have a constant three-dimensional volume then if the specimen is stretched by λ in y-direction then it is contracted by a factor of $\lambda^{-0.5}$ in the x-direction. Let u_y be the displacement in y-direction and L_0 the specimen length. If $\dot{u}$ is the rate of deformation per unit time in y-direction of the specimen then the incremental stretch $d\lambda_y$ in y-direction is given by $\dot{u}\Delta t$, where Δt is the incremental time. Incremental stretch $d\lambda_x$ in x-direction is given by $d\lambda_y / 2\lambda_y^{3/2}$, here λ_y is the stretch in y-direction and is given by relation $1+u_y / L_0$. This ensures that the deformation is volume preserving.

5.4 Defining Strain energy:

The area under the stress-strain curve up to a given value of strain is defined as the strain energy per unit volume consumed by the material in straining it to that value. This is easily shown by the relation,

$$U = \frac{1}{V}\int PdL = \frac{1}{V}\int_0^{\varepsilon} \sigma d\varepsilon, \qquad (1)$$

where V is the volume of specimen, U is the strain energy, σ and ε are the uniaxial stress and strain respectively. P and L are the load and length of the specimen respectively. The tensile engineering stress in the simulated microscopic network, keeping the volume constant and keeping the assumptions of rubber elasticity is given by the relation,

$$\sigma = \frac{1}{V}\left(\frac{\partial U}{\partial \varepsilon}\right)_{\min}. \qquad (2)$$

The derivative should be carried out at energy minimum with respect to the coordinates of all the internal nodes at each incremental deformation step.

5.5 Van der Waals bonds and their breakage:

We had discussed about Van der Waals forces in the previous chapter. Here we will discuss the phenomenon of the breakage of these Van der Waals bond and show some results for different values of the stiffness of these Van der Waals bonds. The model is based on the Eyring activation rate theory [3], which takes into account the role of weak Van der Waals forces between chains. The network is elongated at a constant rate $\dot{\varepsilon}$ and at temperature T along the y-axis. This causes straining of weak Van der Waals bond which break according to the kinetic theory of fracture [5], at the rate

$$v = \tau \exp\left[-(U - \beta\sigma)/kT\right]. \qquad (3)$$

Here τ is the thermal vibration frequency and U and β are the activation energy and volume respectively. σ is the local stress and satisfies the relation $\sigma = \frac{1}{\alpha} K\varepsilon$, where ε is the local strain and K is the elastic constant of the bond, k is the Boltzman's constant and T is the deformation temperature. The quantity α is given by the relation [1,2]

$$\alpha = (n/3)N^{1/2}. \qquad (4)$$

Here N is the number of statistical chain segment and l is their length, n is the number of chain strands per unit volume.

As the Van der Waals bond break the external load is transferred to now effectively isolated chain strand. The simulation of the Van der Waals bond breaking is performed with the help of a Monte Carlo lottery that breaks a bond i according to the probability

$$P_i = v_i / v_{\max}. \tag{5}$$

Here $v_{\max}$ is the rate of breakage of the most strained bond in the array. After each visit of a bond, the time t is incremented by $1/[v_{\max} n(t)]$, where $n(t)$ is the total number of intact bonds at time t. For analysis [1,2] τ was taken to be $10^{12}/s$. We have chosen a displacement increment of 10^{-10} m per time step. Deformation temperature (T) is taken to be 300 K. We have chosen [1,2] U=100 kJ/mol, and $\beta = (26\overset{0}{A})^3$, $n = 3.04\times10^{26}/m^3$ and N= 5. Results for different values of K are shown in the figures below.

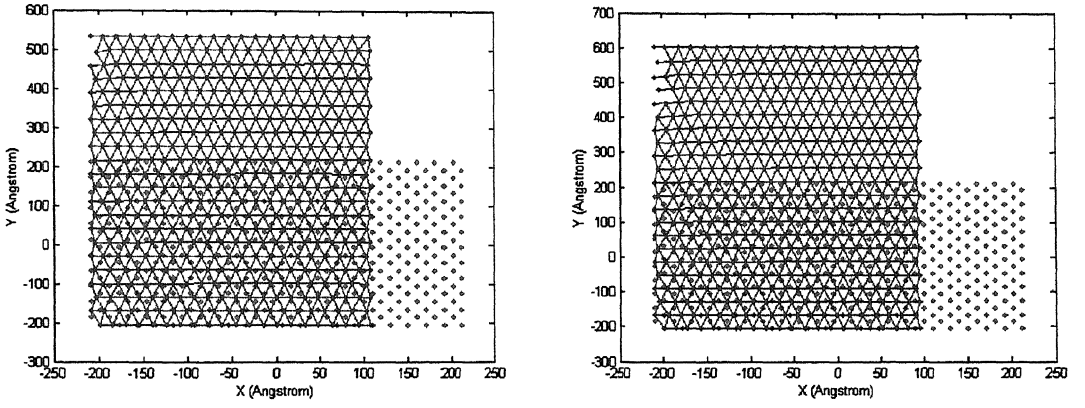

(a) (b)

Figure 1 Deformed polymer for only Van der Waals bond and K=1MPa

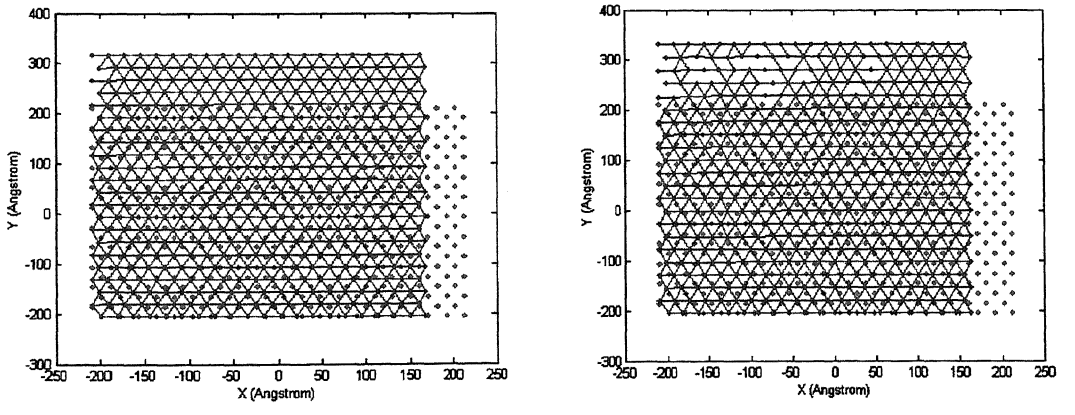

(a) (b)

Figure 3 Deformed meshes for only Van der Waals bond and K=4 MPa

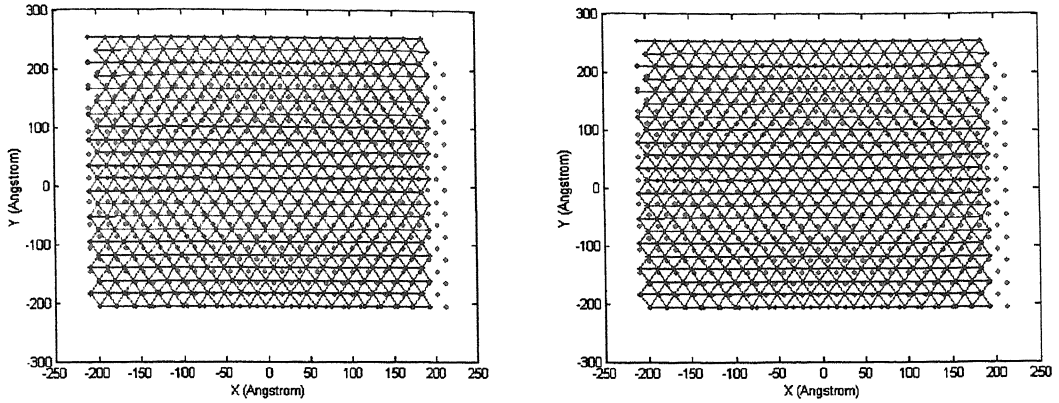

(a) (b)

Figure 4 Deformed meshes for only Van der Waals bond and K=10 MPa

Figure 2 shows deformed shapes of the polymer model with only Van der Waals bond, Stiffness (*K*) of the bonds is taken equal to 1 MPa. The Figure 2(a) shows the shape of the polymer when the breakage of Van der Waals bond just starts (80% strain) and the Figure 2(b) shows the shape of polymer when some of the bonds are broken (90% strain). The undeformed mesh is shown by dots in the background.

Figure 3 shows the deformed meshes of polymer model with only Van der Waals bonds and stiffness (*K*) of bond equal to 4 MPa. Figure 3(a) shows the deformed mesh when the Van der Waals bonds just start breaking at a much lower strain than the case when K=1 MPa (25% strain) and Figure 3(b) shows the deformed mesh when some of the bonds are broken (27% strain).

Figure 4 shows deformed meshes for polymer model with only Van der Waals bond and stiffness (*K*) of bonds equal to 10 MPa. Figure 4(a) shows the deformed mesh when bonds just start to break and Figure 4(b) shows the deformed mesh when some of the bonds are broken. For above value of stiffness the entire bonds break nearly at the same time as due to high stiffness the model behaves like a brittle material and fails without much deformation. As the stress-strain relation is linear for Van der Waals bonds the model with only Van der Waals bond deform in a regular manner.

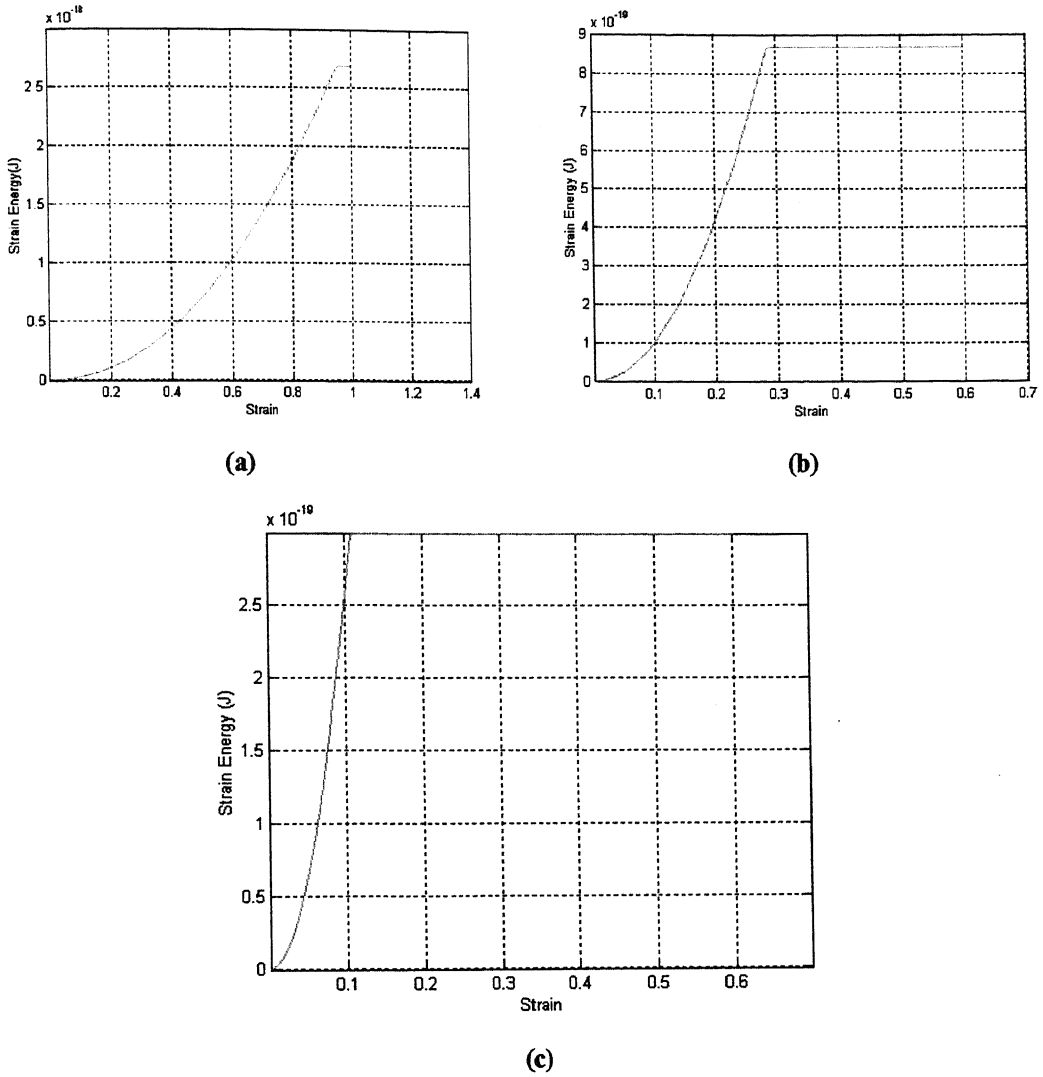

Figure 5 Strain Energy-Strain curve for meshes with only Van der Waals bond and K=1 MPa, K=4 MPa and K=10 MPa respectively

Figure 5 shows the Strain Energy-Strain curve of polymer with only Van der Waals bonds and for stiffness values K=1 MPa [Figure 5(a)], K=4 MPa [Figure 5(b)], K=10 MPa [Figure 5(c)]. From 5(a) it can be seen that after 95% strain the curve flattens out indicating that all the Van der Waals bonds are broken. This flattening of Strain Energy-Strain curve is obtained after 30% and 10% strain for K=4 MPa and K=10 MPa respectively. As the stiffness of the Van der Waals bonds is increased the model becomes stiffer and the bonds break at lower strain. This behavior is shown by the curves obtained for different values of stiffness of Van der Waals bond.

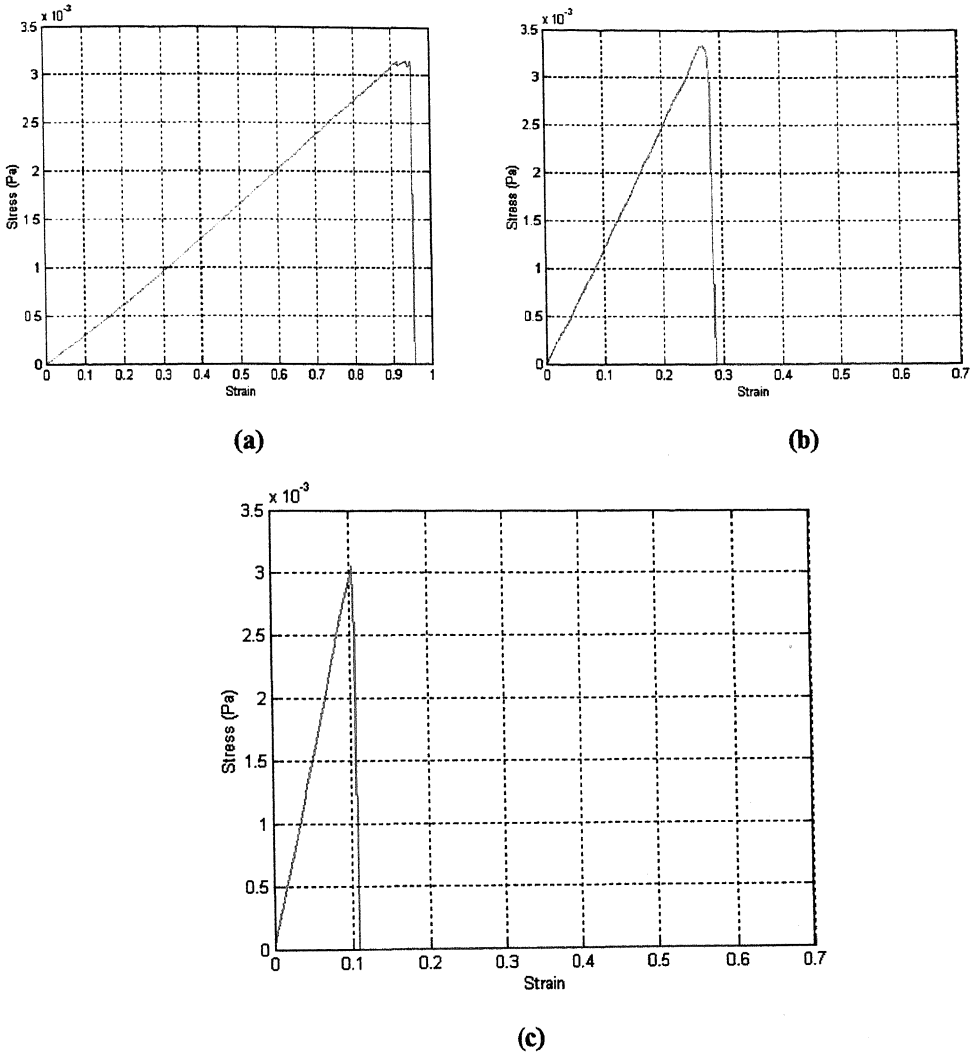

Figure 6 Stress-Strain curve for meshes with only Van der Waals bond and K=1 MPa, K=4 MPa and K=10 MPa respectively

Figure 6 shows the Stress-Strain curve of polymer with only Van der Waals bonds and for stiffness values K=1 MPa [Figure 6(a)], K=4 MPa [Figure 6(b)], K=10 MPa [Figure 6(c)]. The abrupt drop of stress to zero at particular value of strain for various stress-strain curves indicates that at this point entire Van der Waals bonds are broken. As the value of stiffness increases the slope of stress-strain curve also increases. It is clear from the curves that the Van der Waals bonds with less stiffness value can sustain larger deformation than the bonds that are more stiff.

5.6 Strands and their breakage:

As discussed in chapter 3 and chapter 4 strands that are stretched uniaxialy follow the relation

$$f = \frac{kT}{l} L^{-1}(r/Nl). \tag{6}$$

Here f is the force in a strand; l is the length of statistical chain segment is taken to be $10\,\text{Å}$ [1,2]. For variable x we have approximated the Inverse Langevin function by the relation $L^{-1}(x) = x(3-x^2)/(1-x^2)$. Clearly as $x \to 1$ the function $L^{-1}(x) \to \infty$. Plots for N= 5, 12, 20 are shown below. Here no Van der Waals bonds are considered, mesh consists only of strands. Since the stress function depends upon inverse Langevin Function hence the strain energy-strain curve shows a steep increase with strain. The stress-strain relation is also non-linear. Polymer model is deformed to 30% and 60% strain and are the deformed meshes are plotted. The final strain energy-strain curve and stress-strain curve is obtained for 60% strain. At this value of strain the most of the molecular bonds are broken; we break a strand when the draw ratio of the strand approaches $\sqrt{N}$ [19] as at this value of draw ratio the stress approaches infinity ($\sigma \to \infty$).

Figures 7(a & b), 8(a & b) and 9(a & b) show the deformed meshes for polymer model with only strands and number of statistical chain segments (N) equal to 5,12 and 20 respectively. The two deformed meshes for each figure are plotted for 30% and 60% strain respectively. At 30% strain some of the strands are broken and later on most of the strands break giving rise to material failure. The strand is assumed to be broken when its draw ratio approaches a value of $\sqrt{N}$. As can be seen from deformed meshes that as value of N increases less number of strands are broken for same strain value this is due to the fact that at these strain value the strands having higher value of N don't attain the draw ratio of $\sqrt{N}$.

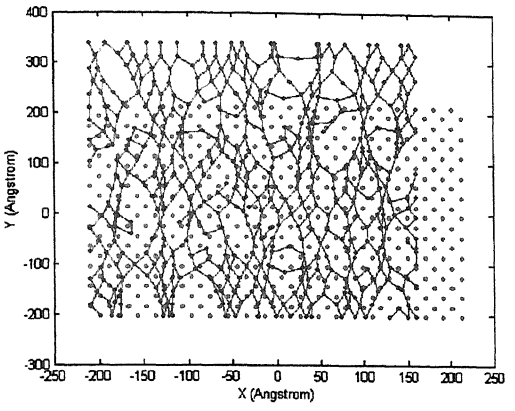

(a)

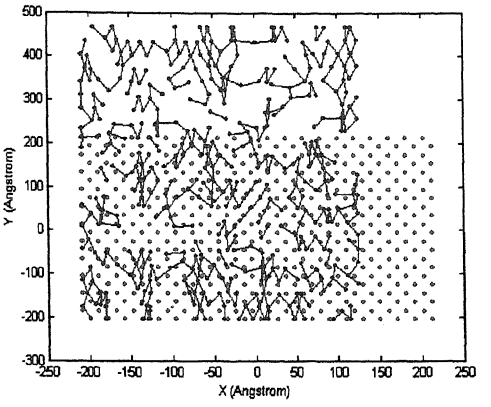

(b)

Figure 7 Deformed meshes after 30% and 60% strain respectively for N=5

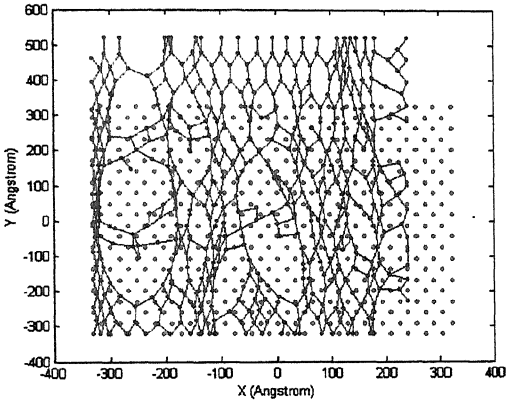

(a)

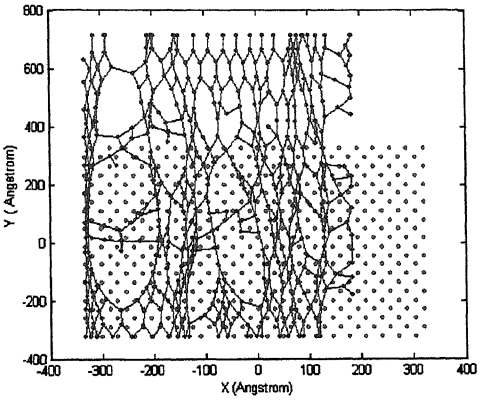

(b)

Figure 8 Deformed meshes after 30% and 60% strain respectively for N=12

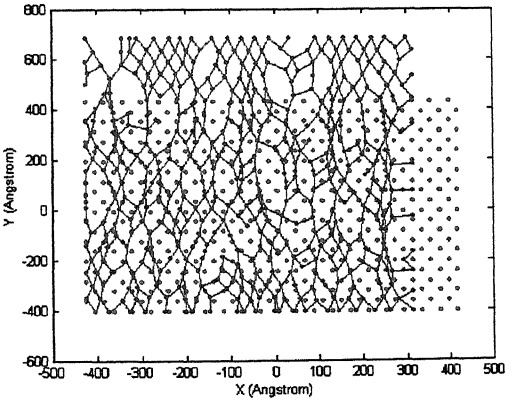

(a)

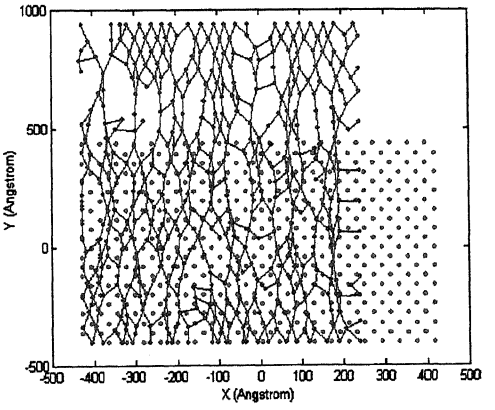

(b)

Figure 9 Deformed meshes after 30% and 60% strain respectively for N=20

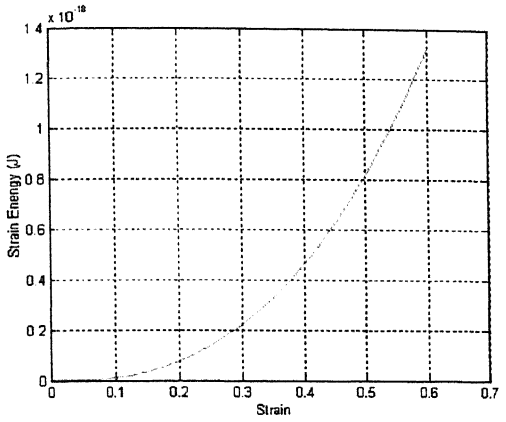

(a)

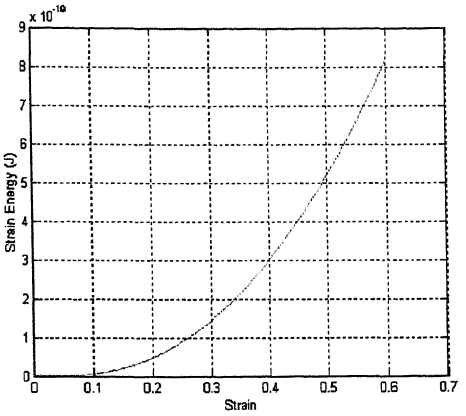

(b)

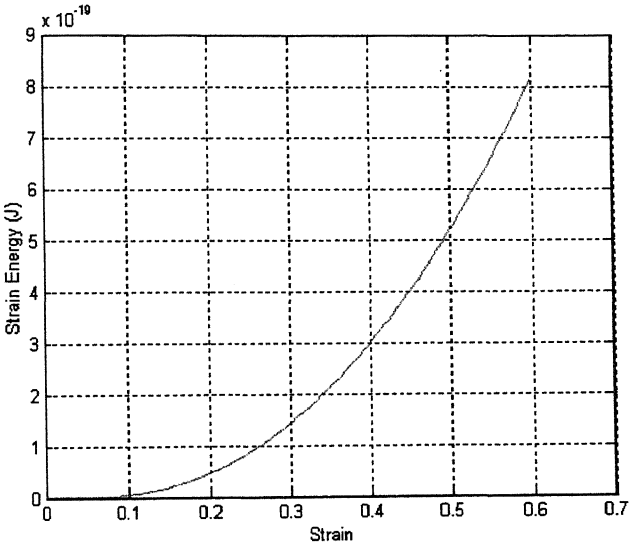

(c)

Figure 10 Strain Energy-Strain curve for meshes with only strands and N=5, N=12, N=20 respectively

Figure 10(a, b, c) shows the Strain Energy-Strain curve for polymer model with only strands and number of statistical chain segments (N) equal to 5,12 and 20 respectively. Strain Energy is a function of Inverse Langevin function hence the curve of strain energy-strain is expected to be as obtained and hence the curve is non-linear in nature. The polymer models were deformed to 60% strain to get these plots.

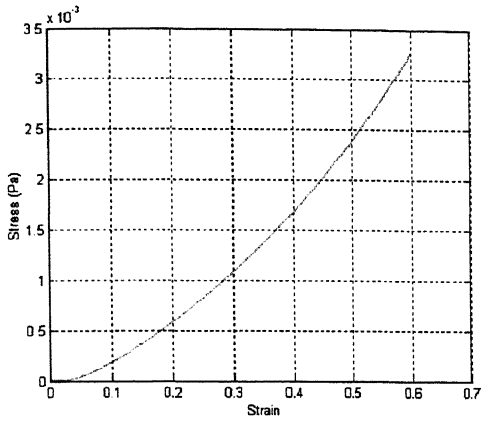

(a)

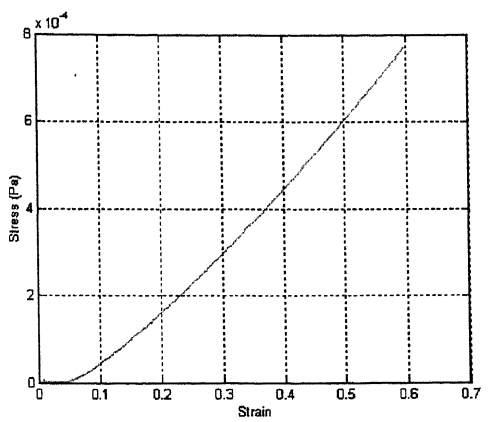

(b)

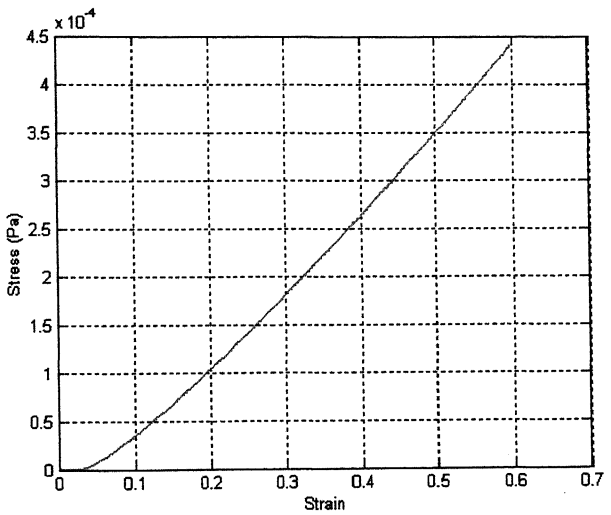

(c)

Figure 11 Stress-Strain curve for meshes with only strands and N=5, N=12, N=20 respectively

Figure 10(a, b, c) shows the Strain Energy-Strain curve for polymer model with only strands and number of statistical chain segments (N) equal to 5,12 and 20 respectively. The Stress-Strain curve is non-linear in nature and as the number of statistical chain segments are increased from 5 to 20 the polymer model attains less maximum stress for same strain value also the non-linearity of the stress-strain curve decreases with the increase in N.

5.7 Actual polymer model with both Strands and Van der Waals forces:

Now results are obtained for both strands and Van der Waals bonds present in the model. Due to Van der Waals force we get the first portion (1) of stress-strain curve in Figure 1 as nearly linear then as the Van der Waals bonds start breaking we get the softening part (2) of the curve and finally for large strain we get the strain hardening part (3). In these following analysis K=4 MPa is kept constant and N is varied.

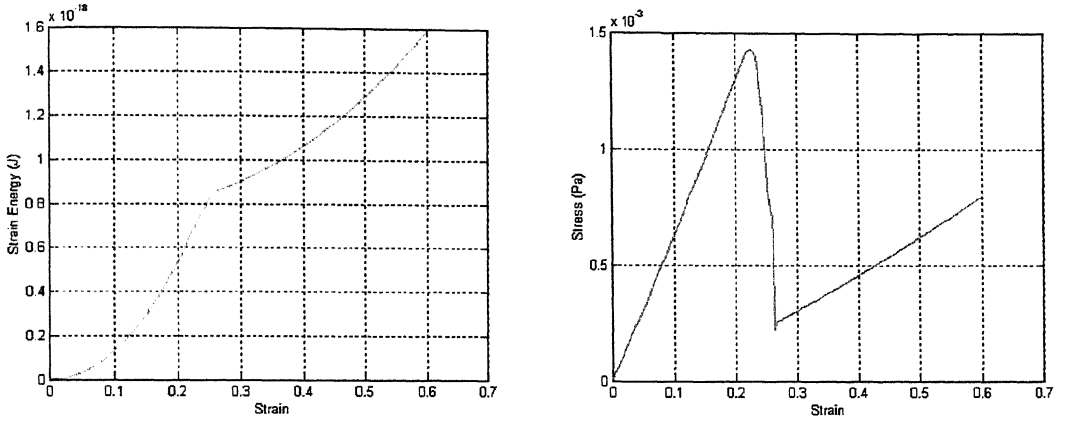

Figure 12 Strain energy-strain and stress-strain curve for N=12 and K=4MPa

Figure 12 shows the strain energy-strain curve and stress-strain curves for polymer model with both Van der Waals bonds and molecular strands present with N=12 and stiffness (K) equal to 4 MPa. From the stress-strain curve it can be seen that up to around 20% strain Van der Waals bonds do not break and at 27% strain all Van der Waals bonds are broken. After breaking of Van der Waals bonds strain hardening of the polymer takes place.

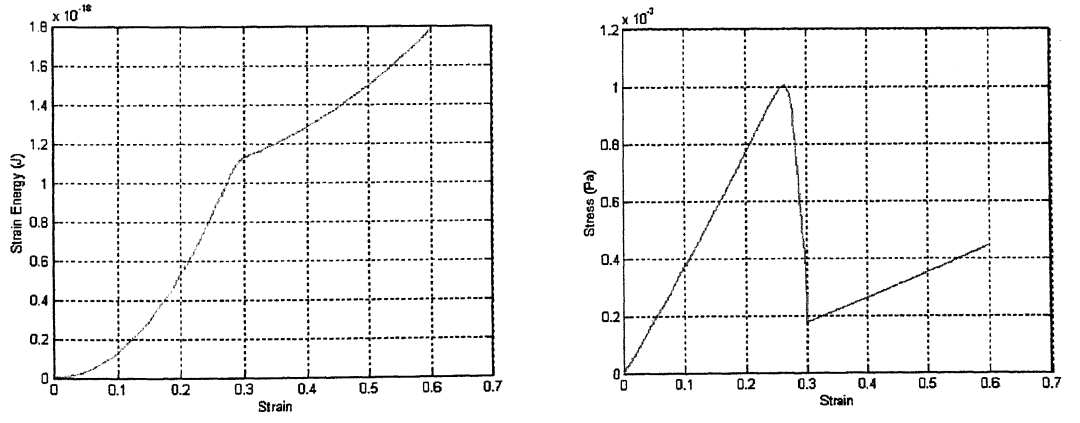

Figure 13 Strain energy-strain and stress-strain curve for N=20 and K=4MPa

Figure 13 shows strain energy-strain and stress-strain curves for polymers model with both Van der Waals bonds and molecular strands present with N=20 and stiffness (K) equal to 20 MPa. Van der Waals bonds start breaking at around 25% strain and all the bonds are broken at 30% strain. Stress at same value of strain for N=20 is less than stress for N=12 which is expected behavior following the curves which were obtained only for strands.

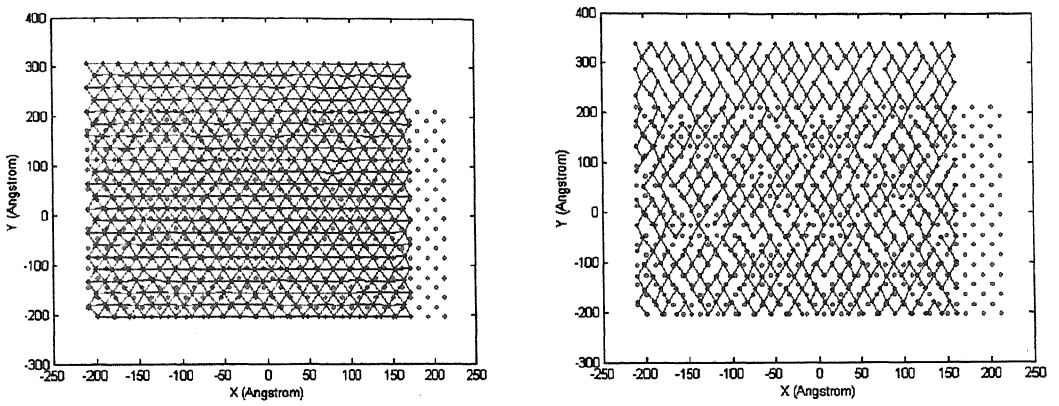

Figure 14 Deformed meshes when all the Van der Waals bonds are present and when all the Van der Waals bonds are broken for N=5 and K=4 MPa

Figure 14 shows the deformed meshes for polymer model with Van der Waals bonds and strands present. N=5 and K=4 MPa is taken, the left hand side figure shows the deformed mesh when all the Van der Waals bonds are present (25% strain) and the right hand side figure shows the deformed mesh when all the Van der Waals bonds are broken (30% strain). It can be seen in Figure 16 that due to presence of Van der Waals bonds the polymer model deforms in a regular fashion and as the Van der Waals bonds are broken the deformation of polymer is in an irregular fashion as can be seen from Figure 17. In Figure 15 the polymer is deformed up to 60% strain. In this figure it can be seen that most of the strands are broken.

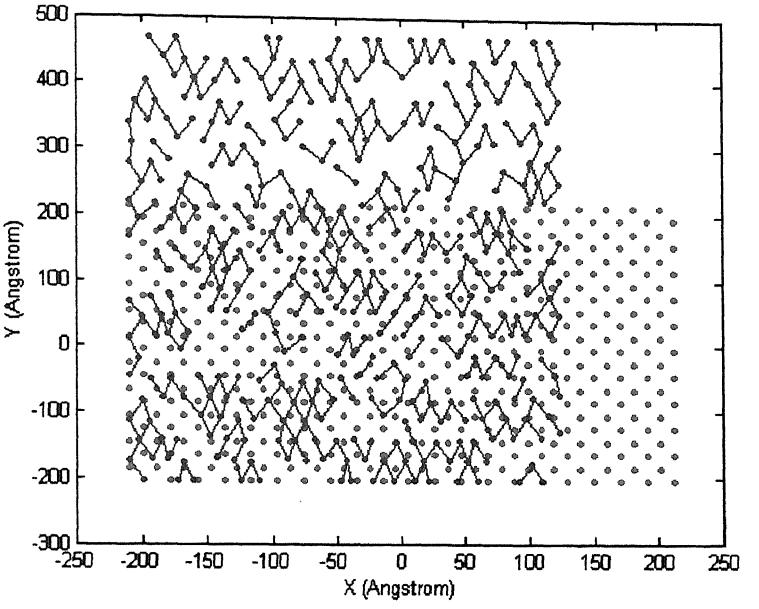

Figure 15 Deformed mesh after 60% strain for N=5 and K=4 MPa

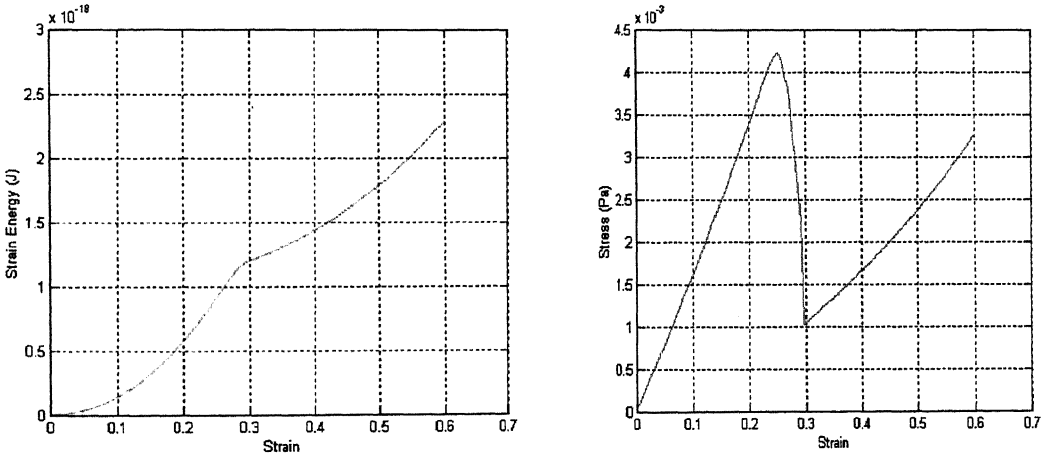

Figure 16 Strain energy-strain and stress-strain curve for N=5 and K=4MPa

Figure 16 shows the strain energy-strain and stress-strain curves for polymer with Van der Waals bonds and strands present. N=5 and K=4MPa is taken for the analysis of the polymer model.

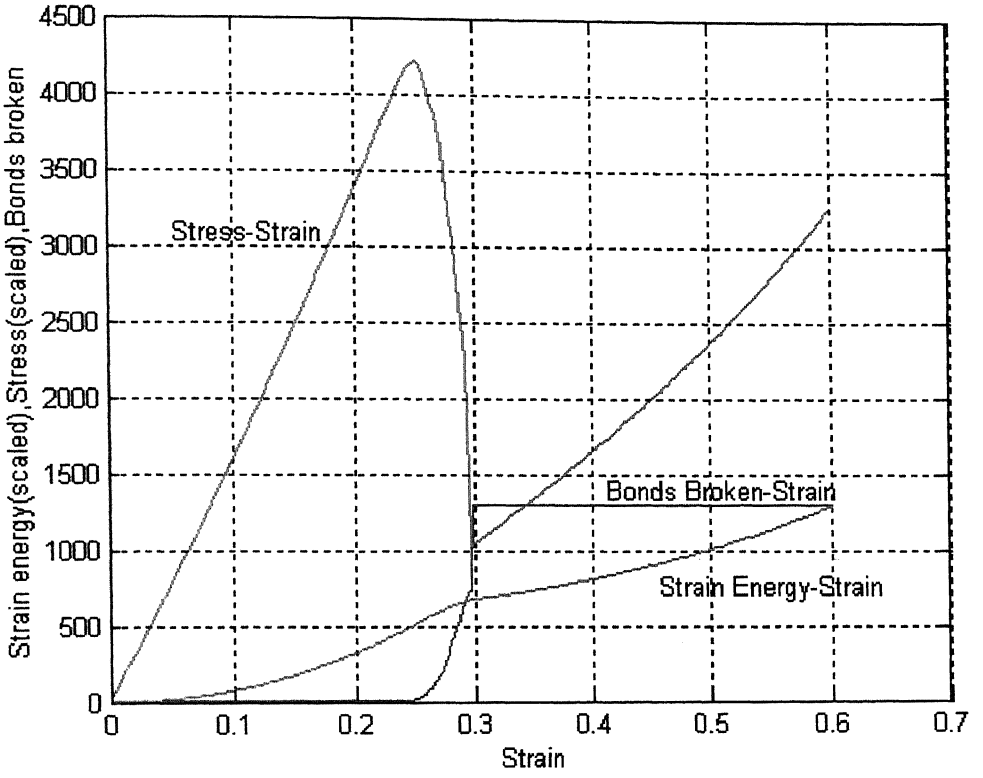

Figure 17 Plot showing Stress-Strain, Strain Energy-Strain, Number of Van der Waals bonds broken-Strain for N=5 and K=4 MPa

Figure 17 shows the plot for Stress-Strain, Strain Energy-Strain, Number of Van der Waals bonds broken-Strain for N=5 and K=4 MPa. From the plot it is clear that the strain hardening starts when all the van der Waals bonds are broken here also the curve of strain energy-strain curve slope changes.

CHAPTER6: CONCLUSION

A model is proposed for deformation of glassy amorphous polymers and the analyze of the same is done using Finite Element Analysis. The parametric data is taken from the reference papers and the results qualitatively mimic the actual behavior of amorphous polymers.

6.1 Scope for future work

As the data for analysis of the polymer model (for example the data taken in the equation of the breakage of Van der bonds using kinetic theory of fracture) is taken from reference papers attempt should be made to verify data from experimentation. Moreover atomistic analyze can be used for better understanding of the Van der Waals bond breakage phenomenon.

We have done a qualitative analysis of the polymer model which can predict the nature of the stress-strain behavior of the actual model, but the values of stresses at a particular strain value do not match with the actual stress value of a polymer under study. Hence the model should be extended to do a quantitative analysis.

Reference:

1. Y. Termonia and P. Smith (1987). Kinetic Model for Tensile Deformation of Polymers. Effect of Molecular Weight. *Macromolecules, **20,** 835-838.*
2. Y. Termonia and P. Smith (1988). Kinetic Model for Tensile Deformation of Polymers. Effect of Entanglement Spacing. *Macromolecules, **21,** 2184-2189.*
3. S. Glassstone, K.J. Laidler and H. Eyring (1941). The Theory of Rate Processes. *McGraw-Hill, New York.*
4. L.R.G. Treloar (1958). The Physics of Rubber Elasticity. *2nd edition; Clarendon: Oxford.*
5. A.S. Krausz and H. Eyring (1975). Deformation Kinetics. *John Wiley & Sons, New York.*
6. W.F. Busse (1932). Physical Structure of elastic Colloids. *J. phys. Chem, **36,** 2862.*
7. W. Kuhn (1934). The Shape of Fibrous Material in Solution. *Kolloidzschr, **68,** 2.*
8. E. Guth and H. Mark (1934). Internal Molecular Statistics, especially in Chain Molecules. *Mh. Chem, **65,** 93.*
9. H. James and E. Guth (1947). Theory of Increase in Rigidity in Rubber during Cure. *Ibid, **11,** 455.*
10. H. James (1947). Statistical properties of networks of flexible chains. *J. Chem. Phys, **15,** 651.*
11. L.R.G. Treloar (1943). The Statistical Length of Paraffin Molecules. *Proc. Phys. Soc.* **55** 345-361.
12. W. Kuhn and F. Grun (1942). Relationship between Elastic Constants and Stretching Double Refraction of Highly Elastic Substances. *Kolloidzschr, **101,** 248.*
13. H.M. James and E.Guth (1943). For a More Recent Extensive Review on the Classical Theories of Rubber Elasticity. *J. Chem. Phys, **11,** 455.*
14. E.M. Arruda and M.C. Boyce (2000). Constitutive Model of Rubber Elasticity; A Review. *Rubber Chemistry and Technology, **73,** 504.*

15. P.D. Wu and Van der Giessen (1993). On Improved Network Models for Rubber Elasticity and their Applications to Orientation hardening in Glassy Polymers. *Journal of Mechanics and Physics of Solid, **41**, 427.*

16. J. Bicerano, N.K. Grant, J.T. Seitz, K. Pant (1997). Microstructural Model for Prediction of Stress-Strain Curves of Amorphous and Semicrystalline Elastomers. *Journal of Polymer Science, **35**, 2715.*

17. T. Belytschko, W.K. Liu, B.Moran (2000). Nonlinear Finite Elements for Continua and Structures. *John Wiley & Sons, New York.*

18. U.W. Gedde (1995). Polymer Physics. *Chapman and Hall.*

19. R.H. Boyd, P.J. Phillips (1993). The Science of Polymer Molecules. *Cambridge University Press.*